Collective and broken pair states of 65,67Ga

Danko, I.; Sohler, D.; Dombradi, Zs.; Brant, Slobodan; Krstić, Vladimir; Cederkall, J.; Lipoglavšek, M.; Palacz, M.; Persson, J.; Atac, A.; ...

Source / Izvornik: **Physical Review C - Nuclear Physics, 1999, 59, 1956 - 1974**

Journal article, Published version
Rad u časopisu, Objavljena verzija rada (izdavačev PDF)

https://doi.org/10.1103/PhysRevC.59.1956

Permanent link / Trajna poveznica: https://urn.nsk.hr/urn:nbn:hr:217:015211

Rights / Prava: In copyright / Zaštićeno autorskim pravom.

Download date / Datum preuzimanja: **2025-03-26**

Repository / Repozitorij:

Repository of the Faculty of Science - University of Zagreb

Collective and broken pair states of ^{65,67}Ga

I. Dankó,[1] D. Sohler,[1] Zs. Dombrádi,[1] S. Brant,[2] V. Krstić,[2] J. Cederkäll,[3] M. Lipoglavšek,[4,5] M. Palacz,[3,6,7] J. Persson,[8] A. Atac,[8] C. Fahlander,[4] H. Grawe,[9] A. Johnson,[3] A. Kerek,[3] W. Klamra,[3] J. Kownacki,[7] A. Likar,[5] L.-O. Norlin,[3] J. Nyberg,[4] V. Paar,[2] R. Schubart,[9] D. Seweryniak,[8,10] D. Vretenar,[2] G. de Angelis,[11] P. Bednarczyk,[11] D. Foltescu,[12] D. Jerrestam,[13] S. Juutinen,[14] E. Mäkelä,[14] B. M. Nyakó,[1] M. de Poli,[11] H. A. Roth,[12] T. Shizuma,[15] Ö. Skeppstedt,[12] G. Sletten,[15] and S. Törmänen[14]

[1]*Institute of Nuclear Research, Debrecen, Hungary*
[2]*Department of Physics, Faculty of Science, University of Zagreb, Zagreb, Croatia*
[3]*Department of Physics, Royal Institute of Technology, Stockholm, Sweden*
[4]*The Svedberg Laboratory, Uppsala University, Uppsala, Sweden*
[5]*J. Stefan Institute, Ljubljana, Slovenia*
[6]*Sołtan Institute for Nuclear Physics, Świerk, Poland*
[7]*Heavy Ion Laboratory, University of Warsaw, Warsaw, Poland*
[8]*Department of Radiation Sciences, Uppsala University, Uppsala, Sweden*
[9]*Gesellschaft für Schwerionenforschung, Darmstadt, Germany*
[10]*Institute of Experimental Physics, University of Warsaw, Warsaw, Poland*
[11]*Laboratori Nazionali di Legnaro, Padova, Italy*
[12]*Chalmers University of Technology, Gothenburg, Sweden*
[13]*Department of Neutron Research, Uppsala University, Nyköping, Sweden*
[14]*Department of Physics, University of Jyväskylä, Jyväskylä, Finland*
[15]*Niels Bohr Institute, University of Copenhagen, Copenhagen, Denmark*

(Received 20 November 1998)

Excited states of ^{65}Ga and ^{67}Ga nuclei were populated through the ^{12}C(^{58}Ni,αp) and ^{12}C(^{58}Ni,$3p$) reactions, respectively, and investigated by in-beam γ-ray spectroscopic methods. The NORDBALL array equipped with a charged particle ball and 11 neutron detectors was used to detect the evaporated particles and γ rays. The level schemes of ^{65,67}Ga were constructed on the basis of $\gamma\gamma$-coincidence relations up to 8.6 and 10 MeV excitation energy, and $I^{\pi}=27/2$ and $33/2^{+}$ spin and parity, respectively. The structure of ^{65,67}Ga nuclei was described in the interacting boson-fermion plus broken pair model, including quasiproton, quasiproton-two-quasineutron, and three-quasiproton fermion configurations in the boson-fermion basis states. Most of the states were assigned to quasiparticle + phonon and three quasiparticle configurations on the basis of their electromagnetic decay properties. [S0556-2813(99)02004-X]

PACS number(s): 23.20.Lv, 21.10.Hw, 21.60.Fw, 27.50.+e

I. INTRODUCTION

The Ga nuclei have three protons above the $Z=28$ shell closure. The simplest way to interpret their low-lying states is to couple the odd proton to the collective states of the corresponding even-even cores. Even within such a simple approximation the yrast sequence could be described up to spin $9/2^{-}$, but the order of the states above the yrast line was mixed up even in the low-spin region [1]. A more exact treatment of the Ga nuclei can be achieved, if the three protons are handled microscopically taking care for the Pauli principle, too, while the neutron excitations can be collected into a set of phonon states. This kind of description was quite successful, and the direct treatment of the three quasiparticles had visible effects even on the properties of the low-lying states [2]. By exciting the Ga nuclei to higher energies, the role of the broken pair states is increasing, and they can be yrast even at a relatively low energy, as the phonon energy in the Zn core nuclei is relatively high, $\approx$1 MeV, resulting in high-energy multiphonon states. At higher energies the break up of the neutron pairs must also be taken into account. A model which is able to handle an odd nucleon coupled to a general anharmonic vibrator core and an additional pair of nucleons was recently developed [3], and tested by describing of the bands of a deformed nucleus [4]. A real challenge for the nuclear models is a description of a nucleus, where the collective structures are already developed, but they are competing with the single-particle degrees of freedom. Thus, a more stringent test of the model where its strength and possible weak points can be revealed would be an attempt to interpret both the excitation energies and the transition probabilities in a transitional nucleus. Because of the available experimental and theoretical information on the low-spin states, as well as on their complexity at higher spins, the Ga nuclei can serve as the test bed for the model.

The low-lying levels of ^{65,67}Ga were already investigated previously via single nucleon transfer reactions [5], radioactive decay of ^{65}Ge [6] and ^{67}Ge [7], as well as (p,n) reaction [8] and other light ion induced reactions [9]. Information on nuclear properties of higher spin states is available from ^{58}Ni(^{12}C,$\alpha p\gamma$)^{65}Ga, ^{60}Ni(^{7}Li,$2n\gamma$)^{65}Ga [10], and ^{53}Cr(^{16}O,$pn\gamma$)^{67}Ga [11], ^{57}Fe(^{12}C,$pn\gamma$)^{67}Ga [12], as well as, from ^{46}Ti(^{25}Mg,$3pxn\gamma$)^{65,67}Ga [13] reactions. The experimental results achieved so far were summarized in recent Nuclear Data Sheets (NDS) compilations for ^{65}Ga [14] and ^{67}Ga [15]. These measurements led to a fairly well estab-

 ©1999 The American Physical Society

lished level scheme up to 4 MeV and spin 15/2−17/2 and the yrast states have been observed up to the 8613 keV $(31/2^-)$ level in ^{65}Ga and the 6590 keV $(27/2^+)$ level in ^{67}Ga.

The ^{12}C+^{58}Ni reaction was studied in order to clarify the origin of background lines in an experiment devoted to investigations of nuclei in the region of ^{100}Sn [16]. As a by product, a substantial amount of new experimental information on the ^{65,67}Ga nuclei was collected, too. The aim of the present work is to extend the available information on excited states of ^{65,67}Ga in the region where the broken pair states dominate the excitation spectrum, and to test the interacting boson-fermion plus a broken pair model by interpreting the experimental data.

II. EXPERIMENTAL PROCEDURE AND DATA ANALYSIS

The experiment was carried out at the Tandem Accelerator Laboratory of the Niels Bohr Institute in Denmark using the NORDBALL multidetector array [17,18]. A 1.5 mg/cm^2 thick ^{12}C target evaporated onto a 23 mg/cm^2 thick gold backing was bombarded with a 261 MeV beam of ^{58}Ni. The detection of γ rays was performed with 15 Compton suppressed Ge detectors having a total photo peak efficiency of about 1%. The detectors were placed in three rings at angles of 79.1°,100.9°, and 142.6° with respect to the beam direction. In order to help the selection of the nucleus of interest from the numerous ones produced in the reaction the γ rays were measured in coincidence with the charged particles and the neutrons emitted by the ^{70}Se compound nucleus. Light charged particles were detected with a 21-element ΔE-type silicon ball covering about 90% of the total solid angle [19]. The average efficiency for the detection and identification of protons and α particles was about 60% and 40%, respectively. The forward 1π solid angle was covered by the Neutron Wall consisting of 11 liquid scintillator detectors assisting in deducing the neutron multiplicity of each event [20]. The discrimination between γ rays and neutrons detected in the neutron detectors was achieved by combining the pulse shape discrimination technique based on the zero-crossover principle and the time-of-flight method [21,22]. The total neutron detection efficiency was about 24%. The detector setup contained also a γ-ray calorimeter composed of 30 individual BaF_2 crystals for total γ-ray multiplicity and sum energy filtering. Furthermore, the logical OR signal from the BaF_2 detectors provided the time reference for all other signals.

Two different trigger conditions were combined. The first of them required at least two γ rays to be detected in the Ge detectors with maximum time difference of 80 ns and at least one γ ray detected in the BaF_2 calorimeter. The second trigger condition was fulfilled, if at least one Ge detector and one BaF_2 detector fired in coincidence with at least one neutron detected in the liquid scintillators. A total of about 120 million coincidence events were collected and sorted off-line into a set of $\gamma\gamma$ matrices gated by different conditions on the numbers of the detected charged particles and neutrons. For energy and efficiency calibration of the Ge detectors the standard ^{133}Ba and ^{152}Eu radioactive sources were used. In the off-line analysis gain matching and gain correction procedures were applied.

Altogether 22 residual nuclei were populated in the experiment. The yield of the ^{65}Ga and ^{67}Ga nuclei was about 12 and 18%, respectively. For studying the ^{65}Ga nucleus a $\gamma\gamma$-coincidence matrix was created with the requirement that one α particle and one proton were detected in coincidence with the γ rays. In the case of ^{67}Ga the events containing three protons were used to create the $\gamma\gamma$-coincidence matrix. These particle gated matrices contained also the γ rays of ^{62,64}Zn and ^{64,66}Ga since some of the particles were not detected, or due to misinterpretation of particles (e.g., two protons as α particle). The $\gamma\gamma$ matrices were analyzed in detail using a standard gating procedure with the aid of the RADWARE software package [23]. Cleaned total projection spectra from the $1\alpha 1p$ and the $3p$ gated matrices are shown in Figs. 1 and 2, respectively. Typical gated spectra are shown in Figs. 3 and 4.

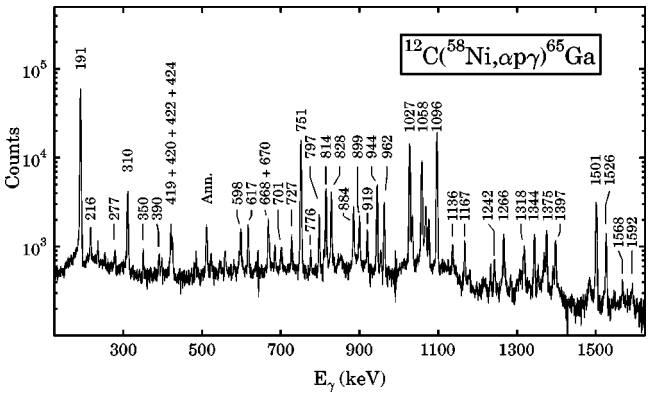

FIG. 1. Total projection spectrum of ^{65}Ga obtained from the $1\alpha 1p$ gated $\gamma\gamma$ matrix after subtraction of the contaminating channels.

The most probable multipolarities were assigned to the transitions on the basis of a simplified $\gamma\gamma$-correlation analysis. The angular distribution ratio

$$R_{\mathrm{ang}}=\frac{I_\gamma(143^\mathrm{o})}{I_\gamma(79^\mathrm{o})+I_\gamma(101^\mathrm{o})}$$

deduced from the intensity of a transition detected at 143° and at 79° or at the equivalent 101° angle relative to the beam direction in coincidence with a γ ray observed at any direction is sensitive to the angular momentum transferred by the γ ray. In order to reduce the uncertainty of the mea-

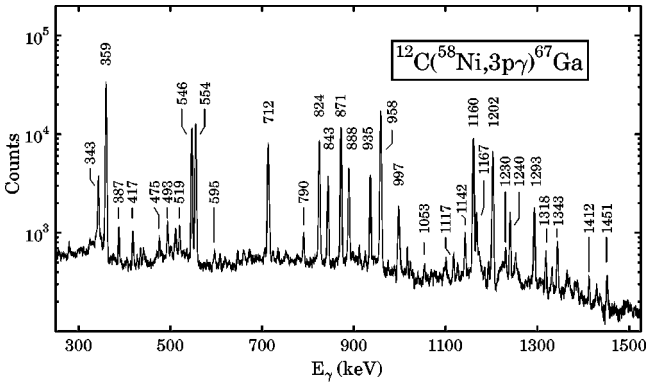

FIG. 2. Cleaned total projection spectrum of ^{67}Ga from the $\gamma\gamma$ matrix obtained by putting a gate on the $3p$ events.

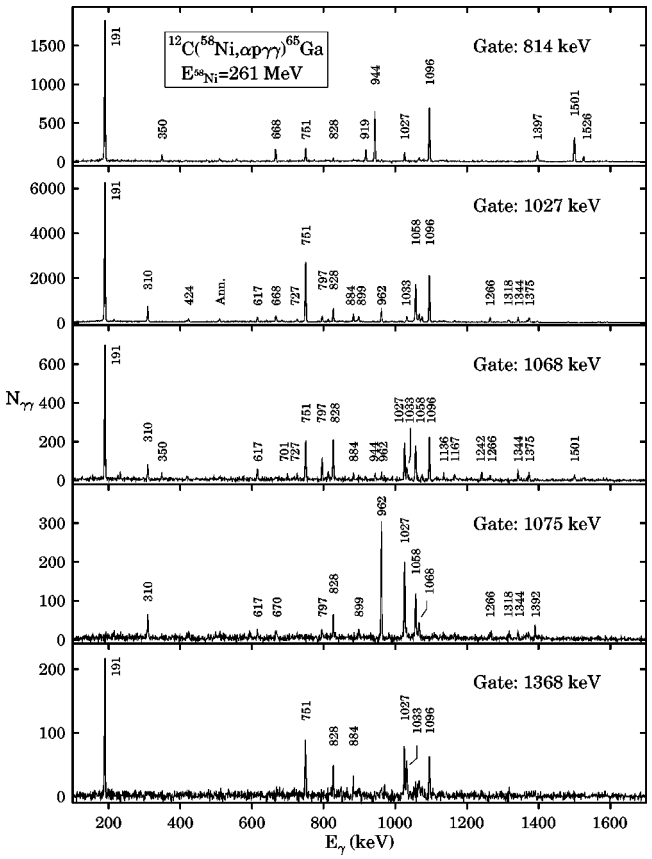

FIG. 3. Typical $\gamma\gamma$-coincidence spectra of ^{12}C(^{58}Ni,αp)^{65}Ga reaction.

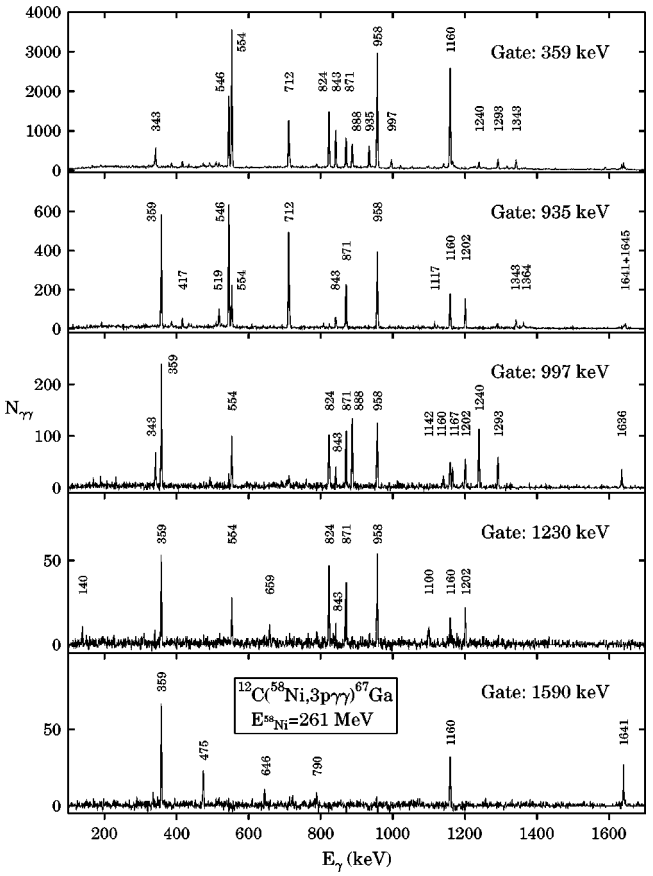

FIG. 4. Typical $\gamma\gamma$-coincidence spectra of the ^{12}C(^{58}Ni,3p)^{67}Ga reaction.

sured $R_{\rm ang}$ values we have taken the weighted average of numerous intensity ratios determined by using different coincident γ rays as gating transitions.

Theoretical $R_{\rm ang}$ values have been calculated previously [24] assuming that transitions of pure multipolarity were emitted from completely aligned initial states. According to that, $R_{\rm ang}\sim 1.5$ corresponds to a stretched quadrupole transition, and $R_{\rm ang}\sim 0.8$ to a stretched dipole one. The measured values are expected to lie between these calculated values and the value of 1 representing the complete attenuation of the alignment. The dependence of $R_{\rm ang}$ on the gating transition was found normally to be smaller than the typical uncertainties in the peak fitting [25]. Furthermore, the fine effects of the angular correlation influenced relatively weakly the $R_{\rm ang}$ ratio because the gating transition was chosen from any of the detectors, and thus both the angle between the two detectors and the angle of the detector relative to the beam direction were integrated over a wide range. In the case of mixed transitions, the $R_{\rm ang}$ varies in the range of 0.3–1.8 depending on the spin difference between the initial and final states and on the mixing ratio δ of the transition [24]. This kind of ambiguity could only be resolved, if a full angular correlation analysis would have been performed on a higher statistics data set. During the multipolarity assignments only $E1$, $M1$, mixed $M1+E2$, and $E2$ transitions were considered. In spite of the fact that the unambiguous determination of the multipolarities of the transitions was not possible, the states were quite often populated or depopulated via different decay paths, which enabled us to assign unique spin to most of the states.

It was also taken into account for spin-parity assignments that in a heavy-ion induced fusion-evaporation reaction high-spin states are populated and the decays mainly proceed via stretched transitions along the yrast line. Thus, the maximum possible spin value allowed by the angular distribution ratios and by the coincidence relationships of the transitions was assigned to the states. Definite parity was assigned to a state if $E2$ or $M1+E2$ multipolarity was determined for one of the deexciting transition, while in the case of $\Delta I=1$ transitions only tentative parities given in parenthesis were ascribed.

III. RESULTS

Tables I and II include the energies, relative intensities, and angular distribution ratios of the ^{65}Ga and ^{67}Ga γ transitions, respectively, together with the deduced spins of the initial and final states. The γ-ray energies and intensities were determined from the $\gamma\gamma$-coincidence matrices. The systematic errors due to the energy and efficiency calibration was estimated to be $\sim$0.3 keV and $\sim$7%, respectively.

On the basis of the measured angular distribution ratios, most of the γ rays could be arranged into two groups. The first group included γ rays having $R_{\rm ang}\leqslant 0.8$ within 1σ uncertainty. The 191 keV transition of ^{65}Ga, depopulating the 191 keV state, was also put into this group in spite of having $R_{\rm ang}=0.85\pm 0.03$ that can be cosidered to be 0.8 only within 2σ uncertainty. These γ rays were assigned to be $\Delta I=1$ transitions (stretched dipole or $M1+E2$ mixed ones). Tran-

TABLE I. Energies, intensities, and angular distribution ratios of γ rays from the ^{12}C(^{58}Ni, $\alpha p \gamma$)^{65}Ga reaction.

E_γ (keV)	I_γ(%)	R ratio	E_i (keV)	$I_i^\pi \rightarrow I_f^\pi$
190.5(3)	100.0(87)	0.85(3)	191	$5/2^- \rightarrow 3/2^-$
216.2(3)	1.5(2)	0.80(9)	4546	$19/2^+ \rightarrow 17/2^+$
277.1(4)	0.3(1)		3064	$13/2^+ \rightarrow 13/2^-$
310.3(3)	6.0(5)	1.30(7)	4432	$17/2^+ \rightarrow 17/2^+$
349.9(3)	0.6(1)	0.73(14)	6293	$23/2 \rightarrow 21/2$
390.3(4)	0.3(1)	0.77(40)	4122	$17/2^+ \rightarrow 15/2^+$
419.0(3)	0.4(1)	1.21(23)	5916	$21/2^+ \rightarrow 21/2^+$
420.2(3)	2.1(2)	0.85(14)	4330	$17/2^+ \rightarrow 15/2^{(+)}$
421.5(4)	0.2(1)		6136	$21/2 \rightarrow 19/2,21/2$
423.8(3)	1.4(1)	0.81(12)	4546	$19/2^+ \rightarrow 17/2^+$
521.9(4)	0.2(1)		6815	$25/2^+ \rightarrow 23/2$
544.2(4)	0.4(1)		1353	$(7/2^-) \rightarrow (5/2^-)$
558.6(4)	0.4(1)		3732	$15/2^+ \rightarrow 11/2^+,13/2^+$
579.5(5)	0.1(1)		6293	$23/2 \rightarrow 19/2,21/2$
594.2(4)	0.4(1)	0.78(34)	4330	$17/2^+ \rightarrow 15/2^{(-)}$
597.8(3)	2.5(2)	1.13(17)	4330	$17/2^+ \rightarrow 15/2^+$
616.5(3)	2.9(3)	0.71(8)	4739	$19/2^{(+)} \rightarrow 17/2^+$
667.5(3)	4.0(3)	0.70(9)	3732	$15/2^+ \rightarrow 13/2^+$
670.1(3)	1.5(2)	0.56(15)	6136	$21/2 \rightarrow 19/2$
684.6(4)	0.8(1)		2037	$9/2^+ \rightarrow (7/2^-)$
700.6(3)	1.2(1)	0.43(15)	4432	$17/2^+ \rightarrow 15/2^+$
727.1(3)	2.1(2)	1.44(10)	5466	$19/2 \rightarrow 19/2^{(+)}$
750.6(3)	53.6(46)	1.28(4)	2037	$9/2^+ \rightarrow 9/2^-$
775.5(3)	1.0(1)		2813	$11/2^{(+)} \rightarrow 9/2^+$
796.9(3)	5.2(5)	0.71(8)	6293	$23/2 \rightarrow 21/2^+$
808.7(4)	0.4(1)		809	$(5/2^-) \rightarrow 3/2^-$
814.2(3)	15.3(14)	1.34(4)	4546	$19/2^+ \rightarrow 15/2^+$
827.8(3)	10.6(9)	1.35(4)	6293	$23/2 \rightarrow 19/2$
833.6(4)	0.3(1)		5466	$19/2 \rightarrow 17/2^+$
845.3(4)	0.7(1)		3910	$15/2^{(+)} \rightarrow 13/2^+$
884.4(3)	9.2(8)	0.70(5)	1075	$7/2^- \rightarrow 5/2^-$
899.1(3)	5.0(5)	1.28(7)	6815	$25/2^+ \rightarrow 21/2^+$
919.0(3)	3.3(3)		3732	$15/2^+ \rightarrow 11/2^{(+)}$
919.5(4)	0.4(1)		5466	$19/2 \rightarrow 19/2^+$
944.1(3)	20.0(17)	0.81(3)	3732	$15/2^+ \rightarrow 13/2^-$
962.1(3)	11.3(10)	0.71(10)	2037	$9/2^+ \rightarrow 7/2^-$
1026.9(3)	60.0(52)	1.31(4)	3064	$13/2^+ \rightarrow 9/2^+$
1033.2(3)	6.0(5)	0.74(5)	5466	$19/2 \rightarrow 17/2^+$
1057.7(3)	38.1(33)	1.36(4)	4122	$17/2^+ \rightarrow 13/2^+$
1063.7(3)	1.6(2)		5496	$21/2^+ \rightarrow 17/2^+$
1067.7(3)	8.8(7)	1.43(15)	7361	$27/2 \rightarrow 23/2$
1075.2(3)	8.0(8)	1.34(9)	1075	$7/2^- \rightarrow 3/2^-$
1096.0(3)	88.8(77)	1.30(3)	1287	$9/2^- \rightarrow 5/2^-$
1097.2(3)	4.6(4)		3910	$15/2^{(+)} \rightarrow 11/2^{(+)}$
1121.8(4)	0.7(1)		3910	$15/2^{(+)} \rightarrow 13/2^-$
1125.2(3)	1.0(1)		7940	$\rightarrow 25/2^+$
1135.3(4)	1.2(2)		3173	$11/2^+,13/2^+ \rightarrow 9/2^+$
1136.0(3)	1.7(2)	0.65(17)	5466	$19/2 \rightarrow 17/2^+$
1162.6(4)	0.6(1)		1353	$(7/2^-) \rightarrow 5/2^-$
1166.8(3)	2.9(3)	1.45(27)	5496	$21/2^+ \rightarrow 17/2^+$
1242.1(3)	1.1(1)		8603	$\rightarrow 27/2$
1265.5(3)	5.7(5)		4330	$17/2^+ \rightarrow 13/2^+$
1268.6(4)	0.6(1)		3736	$15/2^{(-)} \rightarrow 11/2^{(-)}$
1283.5(4)	0.4(1)		5916	$21/2^+ \rightarrow 17/2^+$

TABLE I. (*Continued*).

E_γ (keV)	I_γ(%)	R ratio	E_i (keV)	$I_i^\pi \rightarrow I_f^\pi$
1318.1(3)	3.0(3)		6815	$25/2^+ \rightarrow 21/2^+$
1343.8(3)	5.7(5)	0.73(6)	5466	$19/2 \rightarrow 17/2^+$
1352.9(4)	3.1(9)		1353	$(7/2^-) \rightarrow 3/2^-$
1368.2(3)	2.8(3)		4432	$17/2^+ \rightarrow 13/2^+$
1374.5(3)	6.9(6)	1.36(8)	5496	$21/2^+ \rightarrow 17/2^+$
1391.7(3)	1.8(2)		2467	$11/2^{(-)} \rightarrow 7/2^-$
1397.4(3)	4.9(5)	0.73(10)	5943	$21/2 \rightarrow 19/2^+$
1483.0(4)	0.6(1)		5916	$21/2^+ \rightarrow 17/2^+$
1501.0(3)	19.8(17)	1.33(5)	2788	$13/2^- \rightarrow 9/2^-$
1526.2(3)	8.2(7)	0.73(7)	2813	$11/2^{(+)} \rightarrow 9/2^-$
1567.7(3)	1.3(1)		4632	$17/2^+ \rightarrow 13/2^+$
1591.8(4)	1.0(1)		5714	$19/2,21/2 \rightarrow 17/2^+$
1784.6(4)	0.5(1)		6523	$\rightarrow 19/2^{(+)}$
1793.6(3)	3.4(3)	1.29(12)	5916	$21/2^+ \rightarrow 17/2^+$
1847.0(3)	1.5(2)		2037	$9/2^+ \rightarrow 5/2^-$

sitions in the other group have $R_{\rm ang}=1.32$ within 1σ uncertainty in ^{65}Ga (calculated as the weighted average of measured $R_{\rm ang}$ values of known $\Delta I=2$ transitions of 1027, 1058, 1075, 1096, and 1501 keV decaying from the 3064, 4122, 1075, 1287, and 2788 keV states) and 1.47 in ^{67}Ga (calculated as the weighted average of known $E2$ transitions of 712, 824, 888, 958, 1160, 1167, 1202, 1636 keV depopulating the 4290, 3855, 6379, 3031, 1519, 4198, 1202, and 5491 keV levels). (The lower $R_{\rm ang}$ value for ^{65}Ga is connected to lower alignment of the states in this nucleus which can be explained by the larger angular momentum transferred by the evaporated α particle.) These transitions were assigned to have stretched quadrupole character except for those cases when this assumption led to contradiction. In these cases the overlapping $\Delta I=0$ dipole multipolarity was assigned to them.

In the case of the ^{65}Ga, the 670, 701, and 884 keV γ rays, decaying from the 6136, 4432, and 1075 keV levels, have $R_{\rm ang}$ over 1.5σ less than 0.8, thus they were assigned to be $\Delta I=1$ mixed multipolarity transitions. For the 390 keV γ ray from the 4122 keV state and the 594 keV transition from the 4330 keV state, which have $R\sim 0.8$ but with too high uncertainty ($>20\%$), we could exclude the $\Delta I=2$ stretched quadrupole possibility. We could not deduce multipolarity for the 419, 598, 727, and 1167 keV γ rays, decaying from the 5916, 4330, 5466, and 5496 keV levels, because of the large uncertainties in their $R_{\rm ang}$ values.

In the case of the ^{67}Ga, six transitions could not be placed into one of the above two groups. Three of them, the 546, 843, 1387 keV γ rays, depopulating the 3577, 1202, and 5677 keV states, have $R_{\rm ang}$ over 1.5σ less than 0.8. They were assumed to be $\Delta I=1M1+E2$ transitions. Although, the 925, 1364, and 1714 keV γ rays, decaying from the 4780, 6589, and 2073 keV levels, have $R_{\rm ang}=1.5$, as their uncertainties are too high ($>20\%$) we did not deduce multipolarity for them.

A. Level scheme of ^{65}Ga

The proposed level scheme of ^{65}Ga obtained from the ^{12}C(^{58}Ni,$\alpha p\gamma$) reaction is shown in Fig. 5. All γ rays have been assigned to ^{65}Ga and placed in the level scheme using the $\gamma\gamma$-coincidence relationships. Energy and intensity balances have also been taken into account to confirm the placement of transitions in the level scheme. However, the 2467 and 3173 keV levels are ambiguous due to the uncertain order of the 1392 and 1269 keV, and the 1135 and 559 keV transitions.

Our level scheme is basically consistent with the previous results obtained from heavy-ion induced reactions by Kawakami *et al.* [10] and Zhu *et al.* [13], except for some γ transitions which were replaced or removed on the basis of our coincidence measurement. The most significant deviations from the level scheme of Zhu *et al.* [13] are that the 1794 keV γ ray has been placed below the 899–1125 keV γ cascade and the order of the 1068 and 828 keV γ rays has been changed because of the newly obtained decay branches from the 5916, 6815, and 6293 keV levels. The 900, 1096, and 1392 keV transitions of Banerjee *et al.* [9] were also replaced. In addition, several new levels and transitions have been placed in the level scheme.

The $3/2^-$ spin and parity of the ground state was already established from proton transfer reactions and radioactive decay study of ^{65}Ga. The previously deduced spin-parity values of the 191 keV $5/2^-$, the 1075 keV 7/2, the 1287 keV $(9/2)^-$, the 2037 keV $9/2^+$, the 2788 keV $(13/2^-)$, the 3064 keV $(13/2^+)$, and the 4122 keV (17/2) excited states [14] are strengthened by our angular distribution ratios. Unambiguous spin values could be deduced for the above states, therefore we have adopted these values without parenthesis. In addition, the parity of the 1075 and 4122 keV states has been assigned to be negative and positive, respectively, because of the $E2$ multipolarity assigned to the 1075 and 1058 keV γ rays decaying from them to $3/2^-$ and $13/2^+$ states, respectively. Using these spin-parity values we assigned spins and parities to the other states considering the deduced multipolarities of the transitions and decay properties of the levels.

The group of 2467, 3736, 3910, 4330, 4632, 5496, 5916, and 6815 keV states: The strong 899–1794 keV γ-ray cascade decays through the 5916 keV state from the 6815 keV level leading to the 4122 keV $17/2^+$ state. The angular dis-

TABLE II. Energies, intensities, and angular distribution ratios of γ rays from the ^{12}C(^{58}Ni,3$p\gamma$)^{67}Ga reaction.

E_γ (keV)	I_γ(%)	R ratio	E_i (keV)	$I_i^\pi \rightarrow I_f^\pi$
139.7(5)	0.2(1)		5225	$21/2^- \rightarrow 19/2^{(-)}$
168.8(4)	0.2(1)		3031	$13/2^+ \rightarrow 11/2^+$
278.4(4)	0.5(1)		3855	$17/2^+ \rightarrow 15/2^+$
304.2(4)	0.2(1)		5491	$21/2^+ \rightarrow 21/2^+$
324.0(3)	0.8(1)		4179	$\rightarrow 17/2^+$
328.4(4)	0.1(1)		3190	$11/2^+ \rightarrow 11/2^+$
335.8(7)	0.2(1)		5085	$19/2^{(-)} \rightarrow 17/2^-$
342.5(3)	7.5(7)	1.46(11)	4198	$17/2^+ \rightarrow 17/2^+$
349.1(4)	0.3(1)		5574	$\rightarrow 21/2^-$
358.9(3)	80.4(65)	0.77(3)	359	$5/2^- \rightarrow 3/2^-$
387.1(3)	1.3(1)	1.50(21)	3577	$15/2^+ \rightarrow 11/2^+$
417.4(3)	1.5(2)	0.76(10)	3577	$15/2^+ \rightarrow 13/2^-$
434.3(4)	0.5(1)		4290	$19/2^+ \rightarrow 17/2^+$
441.1(4)	0.3(1)		6185	$(23/2^-) \rightarrow 21/2^{(-)}$
469.9(5)	0.2(1)		4750	$17/2^- \rightarrow 13/2^-, 15/2^-$
475.2(3)	0.8(1)	1.49(22)	5225	$21/2^- \rightarrow 17/2^-$
493.4(3)	1.6(2)	1.49(14)	4349	$17/2^+ \rightarrow 17/2^+$
501.4(4)	0.2(1)		1412	$7/2^- \rightarrow 5/2^-$
519.3(3)	1.7(2)	1.48(12)	5744	$21/2^{(-)} \rightarrow 21/2^-$
526.0(4)	0.4(1)		5751	$\rightarrow 21/2^-$
546.1(3)	38.7(34)	0.62(4)	3577	$15/2^+ \rightarrow 13/2^+$
554.4(3)	44.4(38)	1.45(7)	2073	$9/2^+ \rightarrow 9/2^-$
595.4(4)	0.4(1)		3627	$\rightarrow 13/2^+$
646.1(4)	0.2(1)		5396	$(19/2^-) \rightarrow 17/2^-$
659.3(4)	0.4(1)		5744	$21/2^{(-)} \rightarrow 19/2^{(-)}$
660.2(7)	0.1(1)		2073	$9/2^+ \rightarrow 7/2^-$
705.3(4)	0.4(1)		4995	$21/2^+, 23/2^+ \rightarrow 19/2^+$
712.4(3)	31.8(27)	1.44(8)	4290	$19/2^+ \rightarrow 15/2^+$
715.4(3)	2.6(3)	1.47(17)	3577	$15/2^+ \rightarrow 11/2^+$
789.9(3)	1.0(1)	1.46(16)	6185	$(23/2^-) \rightarrow (19/2^-)$
824.0(3)	41.3(36)	1.46(10)	3855	$17/2^+ \rightarrow 13/2^+$
842.9(3)	15.8(14)	0.60(6)	1202	$7/2^- \rightarrow 5/2^-$
871.3(3)	63.5(55)	0.77(3)	2073	$9/2^+ \rightarrow 7/2^-$
888.4(3)	19.0(17)	1.46(10)	6379	$25/2^+ \rightarrow 21/2^+$
896.2(4)	0.4(1)		5186	$21/2^+ \rightarrow 19/2^+$
910.9(4)	0.2(1)		911	$5/2^- \rightarrow 3/2^-$
924.6(4)	0.6(1)	1.53(63)	4780	$\rightarrow 17/2^+$
935.2(3)	17.3(15)	0.76(5)	5225	$21/2^- \rightarrow 19/2^+$
958.0(3)	100.0(86)	1.45(7)	3031	$13/2^+ \rightarrow 9/2^+$
997.0(3)	5.8(5)	1.50(12)	8616	$33/2^+ \rightarrow 29/2^+$
1022.5(4)	0.8(1)		3884	$\rightarrow 11/2^+$
1053.2(4)	1.0(1)		1412	$7/2^- \rightarrow 5/2^-$
1086.5(6)	0.3(1)		7958	$(27/2^-) \rightarrow 23/2^{(-)}$
1100.0(4)	0.4(1)		6185	$(23/2^-) \rightarrow 19/2^{(-)}$
1116.9(3)	1.1(1)		3190	$11/2^+ \rightarrow 9/2^+$
1126.0(5)	0.4(1)		6870	$23/2^{(-)} \rightarrow 21/2^{(-)}$
1141.7(3)	2.5(2)	1.48(20)	5491	$21/2^+ \rightarrow 17/2^+$
1159.8(3)	61.3(53)	1.48(4)	1519	$9/2^- \rightarrow 5/2^-$
1166.9(3)	8.3(7)	1.50(12)	4198	$17/2^+ \rightarrow 13/2^+$
1172.6(4)	0.8(1)		7552	$\rightarrow 25/2^+$
1183.9(7)	0.6(2)		2596	$\rightarrow 7/2^-$
1193.0(4)	0.6(1)		6379	$25/2^+ \rightarrow 21/2^+$
1202.0(3)	51.7(46)	1.45(7)	1202	$7/2^- \rightarrow 3/2^-$
1219.0(4)	0.6(1)		5417	$\rightarrow 17/2^+$

TABLE II. (*Continued*).

E_γ (keV)	I_γ(%)	R ratio	E_i (keV)	$I_i^\pi \rightarrow I_f^\pi$
1222.6(4)	0.7(1)		7602	$\rightarrow 25/2^+$
1230.0(3)	2.4(3)	0.71(15)	5085	$19/2^{(-)} \rightarrow 17/2^+$
1239.8(3)	6.7(6)	1.48(15)	7619	$29/2^+ \rightarrow 25/2^+$
1292.7(3)	9.4(8)	1.52(14)	5491	$21/2^+ \rightarrow 17/2^+$
1317.7(3)	3.1(3)	1.51(18)	4349	$17/2^+ \rightarrow 13/2^+$
1330.9(3)	1.3(1)	1.48(22)	5186	$21/2^+ \rightarrow 17/2^+$
1343.0(3)	5.3(5)	0.68(9)	2862	$11/2^+ \rightarrow 9/2^-$
1363.8(4)	0.9(1)	1.47(48)	6589	$(25/2^-) \rightarrow 21/2^-$
1368.8(4)	0.6(1)		7958	$(27/2^-) \rightarrow (25/2^-)$
1383.2(5)	0.2(1)		6379	$25/2^+ \rightarrow 21/2^+, 23/2^+$
1387.2(4)	0.6(1)	0.51(20)	5677	$21/2^+ \rightarrow 19/2^+$
1412.2(7)	0.2(1)		1412	$7/2^- \rightarrow 3/2^-$
1451.3(4)	1.9(2)	1.52(24)	2653	$11/2^- \rightarrow 7/2^-$
1467.6(6)	0.4(1)		10084	$\rightarrow 33/2^+$
1540.1(4)	0.6(1)		5396	$(19/2^-) \rightarrow 17/2^+$
1589.9(3)	1.7(2)	1.46(14)	4750	$17/2^- \rightarrow 13/2^-$
1627.2(4)	0.9(1)		4280	$13/2^-, 15/2^- \rightarrow 11/2^-$
1635.5(3)	6.3(5)	1.50(12)	5491	$21/2^+ \rightarrow 17/2^+$
1641.3(3)	4.4(4)	1.47(21)	3160	$13/2^- \rightarrow 9/2^-$
1645.4(4)	1.1(1)	0.85(12)	6870	$23/2^{(-)} \rightarrow 21/2^-$
1714.4(3)	2.3(3)	1.51(36)	2073	$9/2^+ \rightarrow 5/2^-$

tribution ratios measured for the 1794 and 899 keV transitions give $E2$ multipolarities; thus we assigned $21/2^+$ and $25/2^+$ spin-parity values to the 5916 and 6815 keV states, respectively. Another decay branch formed by the 1318–1375 keV γ cascade leads also to the 4122 keV $17/2^+$ state via the 5496 keV state from the 6815 keV level. As the 1375 keV γ ray has $E2$ multipolarity, we assigned $21/2^+$ spin parity to the 5496 keV state also. This assignment is in accordance with the possible $\Delta I=0$ character of the 419 keV transition decaying from the 5916 keV $21/2^+$ state to the 5496 keV state.

The 4330 keV state decays to the 3064 keV $13/2^+$ state via the 1266 keV γ ray and it is fed from the 5496 keV $21/2^+$ state by the 1167 keV transition. As the spin gap is $\Delta I=4$ along the cascade, $I=17/2$ spin is proposed for the 4330 keV state instead of the (15/2) spin proposed previously [14]. Similarly, the 4632 keV state decays to the 3064 keV $13/2^+$ state and is fed from the 5916 keV $21/2^+$ state. Because of the $\Delta I=4$ spin gap, $I=17/2$ spin can be assigned to the middle lying 4632 keV state, if we exclude $\Delta I>2$ multipolarity transitions. As the cascade of $M2$ transitions can be excluded by lifetime considerations, positive parity was assigned to the 4330 and 4632 keV states.

The 3736 keV state decays to the 1075 keV $7/2^-$ state through the 2467 keV state via the 1269–1392 keV γ cascade, and it is fed by the 594 keV γ ray from the 4330 keV $17/2^+$ state. As the $R_{\rm ang}$ value of the 594 keV transition allows for 0 or 1 spin change, $I=15/2,17/2$ spin is allowed for the 3736 keV state. The latter value can be excluded, since, assuming only $\Delta I \leqslant 2$ multipolarity transitions, the 1269–1392 keV γ-ray cascade can bridge only a $\Delta I=4$ spin gap to its $7/2^-$ final state; thus we accepted the $I=15/2$ value. This assignment resulted in spin 11/2 for the 2467 keV state lying in the middle of the cascade. The parity of both states was tentatively assigned as negative on the basis of analogy with ^{67}Ga.

The 3910 keV state is connected to the 2813 keV $11/2^{(+)}$ state via the 1097 keV γ ray and populated from the 4330 keV $17/2^+$ state by the 420 keV transition. The angular distribution ratio of the latter transition gave $\Delta I=1$ character, thus 15/2 spin is assigned to the 3910 keV state. Since the $\Delta I>2$ transitions are excluded, it is highly probable that the 1097 keV transition has $E2$ multipolarity leading to tentative positive parity for the 3910 keV state.

The 2813, 3173, 3732, and 4432 keV states: The 5916 keV $21/2^+$ and the 3064 keV $13/2^+$ states are connected through a cascade of γ rays with the 4432 keV state being in the middle position. The connecting transitions are expected to have $E2$ multipolarities resulting in $17/2^+$ spin-parity value for the 4432 keV state. The proposed $17/2^+$ value is in contradiction with the (21/2) value accepted by NDS [14], but it is in accordance with the excitation function measurement of Kawakami *et al.* giving $I \geqslant 17/2$ spin for this state [10].

The 3732 keV state is populated from the 4432 keV $17/2^+$ state via the 701 keV $\Delta I=1$ transition having $M1+E2$ multipolarity, thus $15/2^+$ spin parity was assigned to the 3732 keV state. This assignment is in agreement with the $\Delta I=1$ characteristics of the 668 and 944 keV transitions decaying from the 3732 keV state to spin 13/2 levels.

The 3732 keV $15/2^+$ state decays to the 3173 keV state, which feeds the 2037 keV $9/2^+$ state. As the spin gap is $\Delta I=3$ and $\Delta I>2$ multipolarity transitions are excluded, $I=11/2^+$ or $13/2^+$ spin-parity values are allowed for the 3173 keV state.

The 2813 keV state decays to the 1287 keV $9/2^-$ state through the 1526 keV transition having $\Delta I=1$ characteristics resulting in 11/2 spin for the initial state in agreement

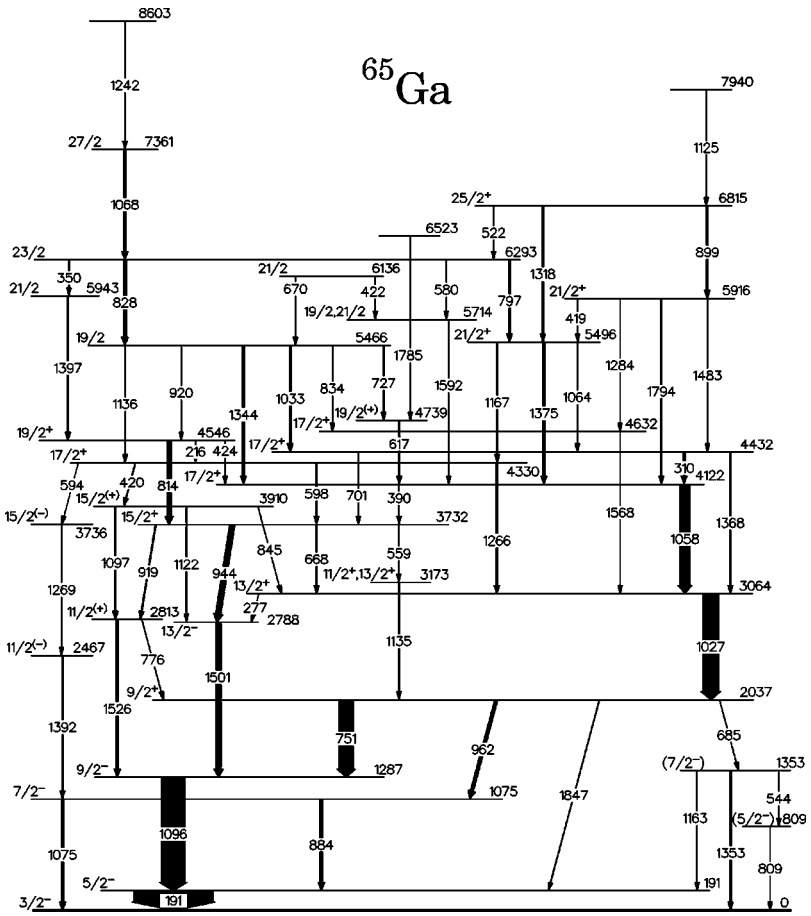

FIG. 5. Proposed level scheme of ^{65}Ga.

with the (11/2) value of the NDS [14]. As the 919 keV transition, feeding the 2813 keV 11/2 state from the 3732 keV $15/2^+$ one, is expected to have $E2$ multipolarity because of the $\Delta I=2$ spin change, tentative positive parity was assigned to the 2813 keV state.

The 4546 keV state: The 4546 keV state decays to the 3732 keV $15/2^+$ state via the 814 keV γ ray having $E2$ multipolarity, and feeds $17/2^+$ states through the 216 and 424 keV transitions having $\Delta I=1$ nature. On this basis $19/2^+$ spin parity was assigned to this state.

The 4739, 5466, and 6136 keV group of states: According to the measured $R_{\rm ang}$ values, the 1033, 1136, and 1344 keV γ rays decaying from the 5466 keV state to 17/2 states have the $\Delta I=1$ nature, thus $I=19/2$ spin was assigned to the 5466 keV state contradicting the previous value of $(25/2^+)$ [13]. The parity of this state is probably positive, because it decays mainly to positive parity states. The 5466 keV state decays via another branch to the 4739 keV state through the 727 keV γ ray, which may have $\Delta I=0$ character according to its $R_{\rm ang}$ value. The 4739 keV state feeds the 4122 keV $17/2^+$ state via the 617 keV γ ray having stretched dipole nature. Thus, $I=19/2^{(+)}$ spin and parity was assigned to the 4739 keV state. The 6136 keV state is established by the 670 keV γ ray decaying to the 5466 keV 19/2 state. The $R_{\rm ang}$ value of this transition gives $\Delta I=1M1+E2$ multipolarity, thus spin 21/2 was assigned to its initial state.

The 5714, 5943, and 6293 keV states: $I=23/2$ spin was assigned to the 6293 keV state on the basis of the $E2$ multipolarity of the 828 keV γ ray decaying from it to the 5466 keV 19/2 state. It is also strengthened by the $\Delta I=1$ nature of the 797 keV transition decaying from it to the 5496 keV $21/2^+$ state. The 5943 keV state is connected to the 4546 keV $19/2^+$ state and to the 6293 keV 23/2 state. Both transitions have $\Delta I=1$ multipolarity, thus 21/2 spin was assigned to this state. The 5714 keV state is established by the 1592 keV γ ray decaying to the 4122 keV $17/2^+$ state and by the 422 and 580 keV γ rays decaying from the 6136 keV 21/2 and 6293 keV 23/2 states, respectively. These decay properties allow $I=19/2,21/2$ spin for the 5714 keV state.

The 7361 keV state: $I=27/2$ spin was assigned to the 7361 keV state according to the $E2$ multipolarity of the 1068 keV transition connecting it with the 6293 keV 23/2 state.

The 809 and the 1353 keV states: We have tentatively assigned $(7/2^-)$ spin-parity value to the 1353 keV state and $(5/2^-)$ spin and parity instead of $1/2^-,3/2^-$ [14] to the 809 keV state, because their decay properties are similar to those of the 1412 and 911 keV states of ^{67}Ga.

B. Level scheme of ^{67}Ga

The proposed level scheme of ^{67}Ga from the ^{12}C(^{58}Ni,$3p\gamma$) reaction is shown in Fig. 6. All γ rays have been placed in the level scheme on the basis of the $\gamma\gamma$-coincidence measurement. Some low-energy γ rays (324, 349, 526, and 595 keV), drawn with dashed lines in the level scheme, have been observed in coincidence with lower-lying transitions of ^{67}Ga. However, their coincidence data were too modest to exclude unambiguously higher energy γ rays below these transitions.

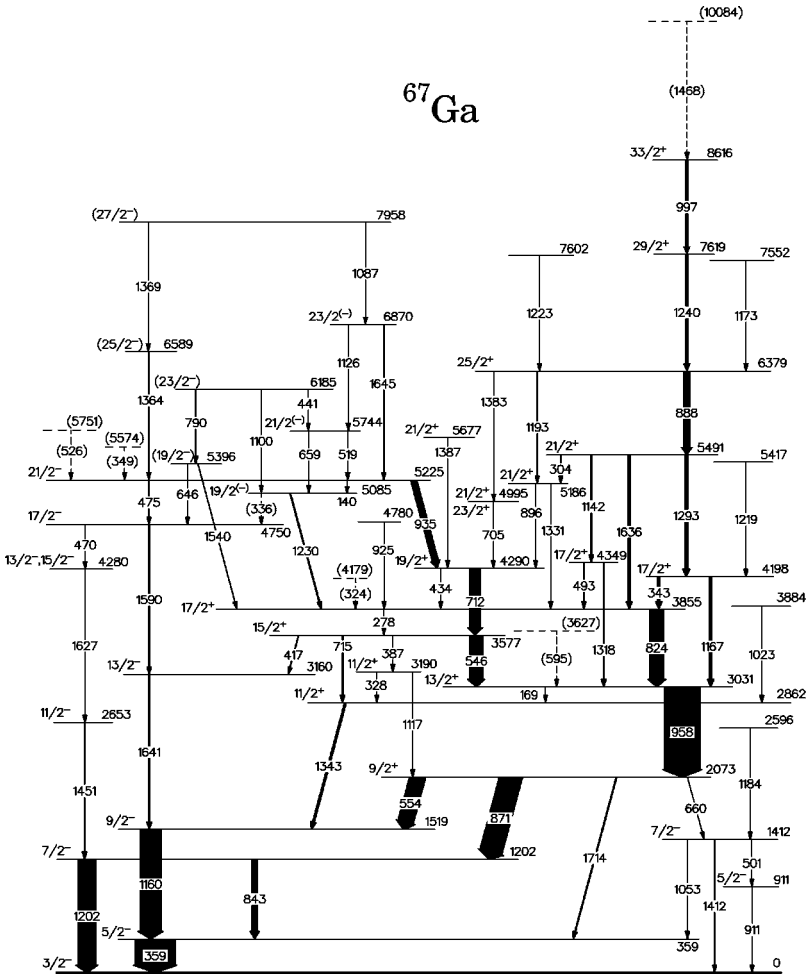

FIG. 6. Proposed level scheme for ^{67}Ga.

Our level scheme is consistent with the previous results obtained from heavy-ion induced reactions by Zobel *et al.* [12] and Zhu *et al.* [13], but our coincidence measurement enabled us to establish several new levels above 3.8 MeV excitation energy.

Beside the $3/2^-$ ground state, spins, and parities of the 359 keV $5/2^-$, 1202 keV $7/2^-$, 1519 keV $9/2^-$, 2073 keV $9/2^+$, 2862 keV $11/2^+$, 3031 keV $13/2^+$, 3190 keV $11/2^+$, 3577 keV $15/2^+$, 3855 keV $17/2^+$, 4198 keV $(17/2^+)$, 4290 keV $19/2^+$, 5491 keV $(21/2^+)$, 6379 keV $(25/2^+)$ excited states have already been known [15]. Our angular distribution ratios strengthen these spin-parity assignments, even in the uncertain cases, thus, the above values were accepted without parentheses. Using the above assignments, we deduced the spin-parity values for the other states, too, on the basis of the angular distribution ratios and the decay properties of the levels. The 911 and 1412 keV states have been excited very weakly in our experiment, their spin-parity values shown in Fig. 6 are adopted values. The spin-parity assignments, which are new, or differing from the previous ones are discussed below.

1. Positive parity states

The 4349 keV state: This state decays via the 493 and 1318 keV γ rays to the 3855 keV $17/2^+$ and to the 3031 keV $13/2^+$ states, respectively. In addition, it is fed from the 5491 keV $21/2^+$ state by the 1142 keV γ ray. According to the $R_{\rm ang}$ ratios, stretched quadrupole, $\Delta I=1$ mixed $M1+E2$ or $\Delta I=0$ dipole multipolarity was determined for all the three transitions. As the 1142–1318 keV γ-ray cascade connect a $21/2^+$ state with a $13/2^+$ state ($\Delta I=4$), both transitions must have stretched quadrupole (i.e., $E2$) multipolarity. Thus, the 4349 keV state has $17/2^+$ spin-parity and the 493 keV transition is a $\Delta I=0$ dipole one in agreement with its $R_{\rm ang}$ value.

The 4995 keV state: This state is in the middle of the 1383–705 keV γ-ray cascade connecting the 6379 keV $25/2^+$ state to the 4290 keV $19/2^+$ state. Both transitions were too weak to get results for their multipolarities. As the spin gap between the initial and final states of the cascade is $\Delta I=3$, excluding $\Delta I>2$ transitions, $21/2^+$ or $23/2^+$ spin-parity values are allowed for the intermediate 4995 keV state.

The 5186 keV state: This state is established by the 1331 keV γ ray populating the 3855 keV $17/2^+$ state, and the 1193 and 304 keV γ rays decaying from the 6379 keV $25/2^+$ and 5491 keV $21/2^+$ state, respectively. As $\Delta I=3$ multipolarity transitions have been excluded, the 1331 and 1193 keV γ rays must be quadrupole transitions to bridge the $\Delta I=4$ spin gap. This is in accordance with the measured $R_{\rm ang}$ ratio of the 1331 keV γ ray. Thus, $21/2^+$ spin-parity value was assigned to the 5186 keV state.

The 5677 keV state: This state was established by the presence of the 1387 keV γ ray on top of the 4290 keV $19/2^+$ state in accordance with Zhu *et al.* [13]. $21/2^+$ spin-parity was assigned to it on the basis of the deduced $\Delta I = 1M1 + E2$ multipolarity.

The 7619 and 8616 keV states: The 7619 keV state was reported previously by Zobel *et al.* [12] to decay by a 1240 keV γ ray to the 6379 keV $25/2^+$ state. An additional γ ray of 997 keV was put on the top of 7619 keV state on the basis of our coincidence relations, leading to the 8616 keV state. From the measured $R_{\rm ang}$ ratio, stretched quadrupole nature was assigned to both γ rays, suggesting $29/2^+$ and $33/2^+$ spin-parity values for the 7619 and 8616 keV states, respectively.

2. Negative parity states

The 2653, 3160, 4280, 4750, and 5225 keV states: The 3160 keV state, decaying via the 1641 keV γ ray to the 1519 keV $9/2^-$ state, has already been proposed previously [11,12]. In the NDS compilation [15], from the 3160 keV state two additional γ rays decaying to the $3/2^-$ ground and to a 1081 keV $1/2^-$ states have been reported. These latter two transitions were obtained only from the radioactive decay of ^{67}Ge [7], while the 1641 keV γ ray was not seen in that experiment. We have seen only the 1641 keV transition in our coincidence spectra when putting a gate on the 1590 and 417 keV γ rays, feeding the 3160 keV state. Thus, it can be concluded that the 3160 keV state is a doublet: one of the levels is a low-spin state, excited only in the decay experiment, and may have $1/2^-$ or $3/2^-$ spin-parity value. The other one, which has been seen from the heavy-ion induced reactions, is a state of $13/2^-$ spin and parity according to the stretched quadrupole nature of the 1641 keV transition, as well as the $\Delta I = 1$ character of the 417 keV γ ray, leading from the 3577 keV $15/2^+$ state to the 3160 keV state.

The 4750 keV state is established by the above-mentioned 1590 keV γ ray, populating the 3160 keV state, and by the 475 keV γ ray decaying from the previously known 5225 keV state. The other branch from the 5225 keV state via the 935 keV γ-ray decaying to the 4290 keV $19/2^+$ state, has already been observed earlier. $(23/2^+)$ spin and parity has been assigned to the 5225 keV state by Zobel *et al.* [12] on the basis of the angular distribution analysis of the 935 keV γ ray. As this transition was contaminated by the 935 keV ^{66}Ga line they applied some correction on the angular distribution coefficients. Our angular distribution analysis based on a particle gated two-dimensional matrix was free from the contamination and gave the $R_{\rm ang} = 0.76(5)$ ratio, resulting in the $\Delta I = 1$ assignment for the 935 keV γ ray. Thus, we propose 21/2 spin value for the 5225 keV state. This assignment is also supported by the fact that stretched quadrupole multipolarity has been obtained for both members of the 475–1590 keV γ-ray cascade connecting the 5225 keV state with the 3160 keV $13/2^-$ sate. The existence of such a cascade excludes the 23/2 spin for the 5225 keV state, and results in $17/2^-$ spin and parity assignment for the intermediate 4750 keV state. The parities of both states are negative, if we assume that the quadrupole transitions are of $E2$ multipolarity. The positive linear polarization value measured for the 935 keV transition by Zobel *et al.* previously, also supports negative parity, if it is a dipole (that is $E1$) transition.

The 2653 keV state, decaying by the 1451 keV transition to the 1202 keV $7/2^-$ state, has already been proposed previously [11]. The newly found 4280 keV state is connected to this state and to the 4750 keV $17/2^-$ one via the 1627 and 470 keV γ rays, respectively. As the 470–1627–1451 keV γ ray cascade connects a $17/2^-$ state to the 1202 keV $7/2^-$ state ($\Delta I = 5$), none of the three transitions can be a $\Delta I = 0$ dipole transition. Thus, the 1451 keV γ ray has to be a stretched quadrupole transition in agreement with its $R_{\rm ang} = 1.52(24)$ value, leading to $11/2^-$ spin-parity value for the 2653 keV state. The 4280 keV state then must have $13/2^-$ or $15/2^-$ spin-parity.

The 5085, 5396, 5744, and 6185 keV states: The $\Delta I = 1$ nature of the 1230 keV γ ray, decaying from the 5085 keV state to the 3855 keV $17/2^+$ one, allows for $I = 19/2$ spin value for its initial state. This assignment is in accordance with the fact that the 5085 keV state is fed from the 5225 keV $21/2^-$ state by a 140 keV γ ray, which is expected to have a dipole character on the basis of its low energy, and relatively high branching ratio.

The 519 keV γ ray, connecting the 5744 keV state to the 5225 keV $21/2^-$ state has either stretched quadrupole or $\Delta I = 0$ dipole character, resulting in $I = 21/2$ or 25/2 spin value for the initial 5744 keV state. The latter possibility can be excluded taking into account the existence of the 659 keV transition leading from the 5744 keV state to the 5085 keV $19/2^{(-)}$ state. Thus, the 21/2 spin value can be assigned to the 5744 keV state.

On the basis of the decay properties of the 5396 and 6185 keV states and the stretched quadrupole character of the 790 keV γ ray between them, we tentatively propose (19/2) and (23/2) spin values for them, respectively.

We have tentatively proposed negative parity for the above group of states as they have more connections to negative parity states than to positive parity ones.

The 6589 keV state: It has already been reported previously by Zobel *et al.* [12] that this state is connected via the stretched quadrupole 1364 keV γ ray to the 5225 keV state. As the spin-parity value of the 5225 keV final state has been changed to $21/2^-$, $I = (25/2^-)$ spin and parity is proposed for the 6589 keV state, instead of the previous $(27/2^+)$ one.

The 6870 keV state: The 1645 keV γ ray from the 6870 keV state to the 5225 keV $21/2^-$ one has $\Delta I = 1$ nature, thus $I = 23/2$ spin was suggested for the 6870 keV state. Tentative negative parity was proposed for this state, since it is connected to other negative parity ones.

The 7958 keV state: It decays to the 6589 keV $(25/2^-)$ and to the 6870 keV $23/2^{(-)}$ states via the 1369 and the 1087 keV γ rays, respectively. Assuming that there is no $\Delta I > 2$ multipolarity transition in the level scheme, $I = (27/2^-)$ spin-parity value is proposed for it.

The 2596, 3884, 4780, 5417, 7552, and 7602 keV states: Each of them was established by one γ ray only. In the absence of measured angular distribution ratio, we were not able to assign spin-parity values to these states.

IV. INTERACTING BOSON-FERMION PLUS BROKEN PAIR MODEL (IBFBPM)

The interacting boson model (IBM) [26,27], the interacting boson-fermion model (IBFM) [28–30] and the interact-

ing boson-fermion fermion model (IBFFM) [31,32] provide a useful framework for the description of nuclear structure in even-even, odd-even, and odd-odd nuclei, respectively. The IBM framework for even-even nuclei was further extended by including broken pairs in addition to the interacting *s* and *d* bosons [33–36]. Analogously, the IBFM for odd-even nuclei has been extended by adding one broken pair [3,4]. This model will be referred to as interacting boson-fermion plus broken pair model (IBFBPM). The IBFBPM and its counterpart for even-even nuclei are used in descriptions of high-spin states. The IBFBPM configuration space of an odd-even nucleus with $2N+1$ valence nucleons comprises

$$|N \text{ bosons} \otimes 1 \text{ fermion}\rangle + |(N-1) \text{ bosons} \otimes 1 \text{ broken pair} \otimes 1 \text{ fermion}\rangle. \tag{4.1}$$

In this way, both the one- and three-quasiparticle states coupled to the boson core are included and mixing between them is accounted for. The IBFBPM Hamiltonian includes four terms: the interacting boson model (IBM) Hamiltonian [26], the boson-fermion interactions of the interacting boson-fermion model (IBFM) [28], the fermion Hamiltonian and a pair-breaking interaction that mixes one-fermion and three-fermion states. The definition of parameters in the IBM and IBFM terms in this article is taken according to Ref. [37], and in the fermion and pair-breaking terms according to Ref. [3].

In the IBFBPM calculation for ^{65,67}Ga we account for broken neutron and proton pairs, i.e., one-quasiproton, one-quasiproton-two-quasineutron, and three-quasiproton states are included in the basis states (4.1). We note that the IBFBPM calculations with broken neutron and proton pairs have to be done separately, due to the prohibitively large configuration space that would include both type of pairs. Therefore, mixing between broken neutron and proton pairs is not accounted for. The IBFBPM Hamiltonian is diagonalized in the basis (4.1):

$$|I_k^{\pi}\rangle = \sum_{j n_d \upsilon R} \xi_{j,n_d \upsilon R;I} \; |\pi\tilde{j}, n_d \upsilon R; I\rangle + \sum_{jj'j''I_{\alpha\alpha}I_{\pi\alpha\alpha} n_d \upsilon R} \eta_{jj'j''I_{\alpha\alpha}I_{\pi\alpha\alpha},n_d\upsilon R;I} \times |[\pi\tilde{j},(\alpha\tilde{j}',\alpha\tilde{j}'')I_{\alpha\alpha}]I_{\pi\alpha\alpha}, n_d \upsilon R; I\rangle. \tag{4.2}$$

Here $\pi\tilde{j}$ stands for a proton quasiparticle, and $\alpha\tilde{j}',\alpha\tilde{j}''$ for neutron quasiparticles ($\alpha=\nu$), or proton quasiparticles ($\alpha=\pi$), which are coupled to the angular momentum $I_{\alpha\alpha}$. Angular momenta j and $I_{\alpha\alpha}$ are coupled to the three-quasiparticle angular momentum denoted by $I_{\pi\alpha\alpha}$. In the boson part of the wave function, the $n_d d$ bosons are coupled to the total boson angular momentum R. The additional quantum number υ is used to distinguish between the n_d-boson states having the same angular momentum R. We note that the number of *s* bosons associated with the boson state $|n_d \upsilon R\rangle$ is $n_s = N - n_d$, where N is the total number of bosons.

V. CALCULATION FOR ^{65}Ga IN IBFBPM

As a continuation of our study of the series of nuclei in the $A \approx 70$ region [38–45], in this paper we investigate the structure of ^{65,67}Ga nuclei. The core parameters adjusted to the low-lying levels of the $^{64}_{30}Zn_{34}$ even-even nucleus: $h_1 = 0.8$, $h_2 = -0.2$, $h_3 = 0$, $h_{40} = 0.1$, $h_{42} = -0.15$, $h_{44} = 0.3$ (all h_i parameters in MeV) and the total boson number $N=4$, corresponding to the number of valence-nucleon pairs, were previously used in the IBM calculation for low-lying states of ^{65}Ga,^{65}Zn and in the IBFFM calculation for ^{66}Ga [39]. This parametrization corresponds to a transition between the SU(5) and O(6) dynamical symmetries, being closer to the SU(5) (vibrational) limit.

As pointed out in Ref. [38], spectroscopic data for odd-even Ga isotopes cannot be accounted for using proton quasiparticle energies and occupation probabilities from standard Kisslinger-Sorensen [46] and Reehal-Sorensen [47] parametrizations. The most appropriate is the parametrization [38] close to the values obtained from a fit to experimental data in Ref. [48]. Therefore, we have taken the energies and occupation probabilities of proton quasiparticles very close to those from Ref. [38]: $E(\pi\tilde{p}_{3/2}) = 0.91$ MeV, $E(\pi\tilde{p}_{1/2}) = 1.61$ MeV, $E(\pi\tilde{f}_{5/2}) = 1.63$ MeV, $E(\pi\tilde{g}_{9/2}) = 4.15$ MeV, $v^2(\pi\tilde{p}_{3/2}) = 0.60$, $v^2(\pi\tilde{p}_{1/2}) = 0.08$, $v^2(\pi\tilde{f}_{5/2}) = 0.05$, $v^2(\pi\tilde{g}_{9/2}) = 0.01$. These values can be obtained from BCS calculations starting from Reehal-Sorensen [47] single-particle energies with additional shifts ($f_{5/2}$ and $g_{9/2}$ being shifted 0.6 and 0.9 MeV up and $p_{1/2}$ 0.6 MeV down). The resulting $E(\pi\tilde{f}_{5/2})$ and $E(\pi\tilde{p}_{1/2})$ quasiparticle energies are lowered by 0.42 and 0.05 MeV, respectively, and $E(\pi\tilde{g}_{9/2})$ is increased by 0.34 MeV.

The quasiparticle energies and occupation probabilities for neutrons have been calculated using single-particle energies and pairing strength from the calculations for ^{65}Zn [39] and ^{65}Ge [43]. The resulting quasiparticle energy $E(\nu\tilde{f}_{5/2})$ was lowered by 0.14 MeV and $E(\nu\tilde{g}_{9/2})$ by 0.8 MeV (as in ^{67}Ge [45]). Therefore, for ^{65}Ga we use: $E(\nu\tilde{f}_{5/2}) = 1.20$ MeV, $E(\nu\tilde{p}_{3/2}) = 1.45$ MeV, $E(\nu\tilde{p}_{1/2}) = 2.37$ MeV, $E(\nu\tilde{g}_{9/2}) = 2.47$ MeV, $v^2(\nu\tilde{f}_{5/2}) = 0.41$, $v^2(\nu\tilde{p}_{3/2}) = 0.71$, $v^2(\nu\tilde{p}_{1/2}) = 0.08$, $v^2(\nu\tilde{g}_{9/2}) = 0.04$.

In the calculation for negative parity states the boson-fermion interaction strengths for protons are [39]: $\Gamma_0^{\pi} = 0.48$ MeV, $\Lambda_0^{\pi} = 1.4$ MeV, $A_0^{\pi} = 0.05$ MeV, $\chi^{\pi} = -0.5$. For positive parity states the monopole strength is reduced to $A_0^{\pi} = 0$ MeV. For neutrons we take $\Gamma_0^{\nu} = 0.02$ MeV, $\Lambda_0^{\nu} = 1.65$ MeV, $A_0^{\nu} = 0$ MeV, $\chi^{\nu} = -1.0$, i.e., the values used in the previous IBFBPM calculation for ^{67}Ge [45].

The values of the pair-breaking interaction strengths U_0, U_2 and the surface δ interaction strength V_{δ} both for protons and for neutrons in broken pairs are taken in accordance with the previous IBFBPM calculations [49,50] and are equal to the values used in the calculations for ^{67}Ge [45]: $U_0 = 0$ MeV, $U_2 = 0.2$ MeV, and $V_{\delta} = -0.1$ MeV.

In Fig. 7 we present the calculated energy spectrum of ^{65}Ga in comparison to the available data. Only states that have tentative experimental counterparts are shown.

Using the IBFBPM wave functions we have calculated

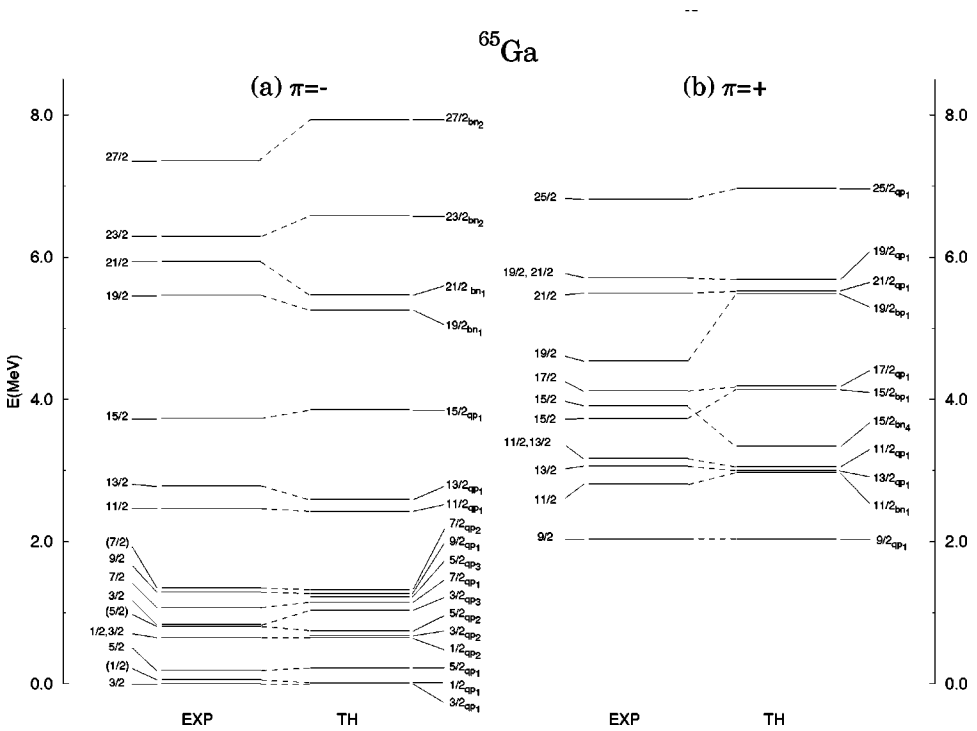

FIG. 7. Calculated states in ^{65}Ga of (a) negative parity and (b) positive parity, in comparison to the available data. Below 1.35 MeV of excitation energy all calculated states are shown, and above 1.35 MeV only those that have experimental counterparts. Calculated states are tentatively assigned to the experimental levels (see text for discussion).

the $E2$ and $M1$ electromagnetic properties. The effective charges and gyromagnetic ratios are taken from the previous IBM/IBFM/IBFFM calculation for ^{64,65,66,67}Zn and ^{65,66,67,68}Ga [38,39]: $e^{\pi}=1.5$, $e^{\nu}=0.5$, $e^{\mathrm{vib}}=1.35$, $\chi=-0.5$, $g_l^{\pi}=1$, $g_l^{\nu}=0$, $g_s^{\pi}=0.4$ $g_s^{\pi,\mathrm{free}}=2.234$, $g_s^{\nu}=0.9$ $g_s^{\nu,\mathrm{free}}=-3.443$, $g_t^{\pi}=\frac{1}{50}\langle r^2\rangle g_s^{\pi,\mathrm{free}}=1.56$, $g_t^{\nu}=\frac{1}{50}\langle r^2\rangle g_s^{\nu,\mathrm{free}}=-1.07$, $g_R=Z/A=0.477$. The calculated $E2$ and $M1$ transitions are compared with the experimental data in Table III. The branching ratios from 21 states were investigated. It was found that all the calculated weak transitions are weak, or were not seen in the experiment. All the transitions expected to be strong are found experimentally, except the $19/2^+_{\mathrm{qp}_1}\rightarrow 15/2^+_{\mathrm{bp}_1}$ transitions, which is predicted to be strong but even so it is below the detection limit. This quality of the description, where the characteristic branches can be understood may serve as a basis for the assignment of the experimental states to the theoretical ones.

To make it easier to follow the origin of states, for the indexing of the theoretical states we use I_{qp_i} for the quasiparticle+phonon states, I_{bp_i} for proton broken pair states and I_{bn_i} for neutron broken pair states. Here the index i denotes the ith state of the denoted type. In the standard notation I_k, the index k is used as total label obtained from the IBFBPM calculation. The indexing I_k is pointed out only for states where $i\neq k$. Otherwise, the indexes i and k are equal.

The lower part of the observed negative parity spectrum is dominated by low-spin parity states, where the $\pi\tilde{p}_{1/2}$, $\pi\tilde{p}_{3/2}$, and $\pi\tilde{f}_{5/2}$ quasiproton states are coupled to the core. The levels at 0, 650, and 809 keV, assigned to the $3/2^-_{\mathrm{qp}_1}$, $1/2^-_{\mathrm{qp}_2}$, and $5/2^-_{\mathrm{qp}_2}$ states respectively, are based on the $\pi\tilde{p}_{3/2}$ state. The IBFBPM states $5/2^-_{\mathrm{qp}_1}$, $9/2^-_{\mathrm{qp}_1}$, $11/2^-_{\mathrm{qp}_1}$, and $13/2^-_{\mathrm{qp}_1}$, based on the $\pi\tilde{f}_{5/2}$ state, are assigned to the levels at 191, 1287, 2467, and 2788 keV, respectively. The level at 62 keV is assigned to the $1/2^-_{\mathrm{qp}_1}$ state having $\pi\tilde{p}_{1/2}$ and $\pi\tilde{f}_{5/2}$ dominant components, while the $\pi\tilde{p}_{3/2}$ and $\pi\tilde{f}_{5/2}$ states are dominant in the $7/2^-_{\mathrm{qp}_1}$, $7/2^-_{\mathrm{qp}_2}$, and $15/2^-_{\mathrm{qp}_1}$ states associated with the experimental levels at 1075, 1353, and 3736 keV, respectively. The level at 815 keV assigned as $3/2^-_{\mathrm{qp}_3}$, as well as the $3/2^-_{\mathrm{qp}_2}$ calculated state, have a more complex structure with components from all the three negative parity quasiproton states. We note that the $1/2^-_{\mathrm{qp}_2}$ assignment to the level at 650 keV is based on the analogy with a similar level in ^{67}Ga; nevertheless its decay properties give a preference for the $3/2^-_{\mathrm{qp}_2}$ assignment. The calculated transitions from the $13/2^-_{\mathrm{qp}_1}$ and $15/2^-_{\mathrm{qp}_1}$ states to all the other calculated states below them that are not observed in experiment are negligible, and from the $11/2^-_{\mathrm{qp}_1}$ state are less than 0.6% of the main branch.

The lowest lying calculated high-spin one-quasiproton states of negative parity $17/2^-_{\mathrm{qp}_1}$, $19/2^-_{\mathrm{qp}_1}$, and $21/2^-_{\mathrm{qp}_1}$ are the $17/2^-_1$, $19/2^-_3$, and $21/2^-_2$ ones. These states are based on the $\pi\tilde{f}_{5/2}$ quasiparticle state, and are predicted to lie at 4105, 5539, and 5721 keV, respectively. According to the IBFBPM calculation, the observed highest spin negative parity one-quasiproton state could be the $17/2^-$ one. This level, corresponding to the level at 4750 keV in ^{67}Ga, was not observed in ^{65}Ga (there is no evidence for a transition of $\approx$1400 keV to the $13/2^-_{\mathrm{qp}_1}$ level).

The lowest lying low-spin negative parity states based on

TABLE III. Calculated $E2$ and $M1$ transitions for ^{65}Ga in comparison to data. Experimental I_γ values for transitions that are not observed in the present experiment are from Ref. [14].

$I_i^\pi \rightarrow I_f^\pi$ ($\hbar$) ($\hbar$)	$E_i \rightarrow E_f$ Expt. Expt.	$B(E2)(e^2\mathrm{b}^2)$ IBFBPM	$B(M1)(\mu_N^2)$ IBFBPM	I_γ Expt.	I_γ IBFBPM
$1/2^-_{qp_1} \rightarrow 3/2^-_{qp_1}$	62→0	0.010	0.043	100	100
$5/2^-_{qp_1} \rightarrow 1/2^-_{qp_1}$	191→62	0.028			3.6
$\rightarrow 3/2^-_{qp_1}$	→0	0.003	0.003	100	100
$1/2^-_{qp_2} \rightarrow 5/2^-_{qp_1}$	650→191	0.001		6	0.4
$\rightarrow 1/2^-_{qp_1}$	→62		0.020	8	99
$\rightarrow 3/2^-_{qp_1}$	→0	0.020	0.009	100	100
$5/2^-_{qp_2} \rightarrow 1/2^-_{qp_2}$	809→650	0.001			0.0003
$\rightarrow 5/2^-_{qp_1}$	→191	2×10^{-5}	0.001	7	0.7
$\rightarrow 1/2^-_{qp_1}$	→62	0.003		6	1.8
$\rightarrow 3/2^-_{qp_1}$	→0	0.035	0.42	100	100
$3/2^-_{qp_3} \rightarrow 5/2^-_{qp_2}$	815→809	0.004	0.098		0.0004
$\rightarrow 1/2^-_{qp_2}$	→650	0.001	0.164		18
$\rightarrow 5/2^-_{qp_1}$	→191	0.004	2×10^{-6}		6
$\rightarrow 1/2^-_{qp_1}$	→62	0.022	0.001	100	100
$\rightarrow 3/2^-_{qp_1}$	→0	0.015	7×10^{-5}	43	94
$7/2^-_{qp_1} \rightarrow 3/2^-_{qp_3}$	1075→815	0.002			0.006
$\rightarrow 5/2^-_{qp_2}$	→809	0.007	0.025		2.2
$\rightarrow 5/2^-_{qp_1}$	→191	0.015	3×10^{-5}	115	26
$\rightarrow 3/2^-_{qp_1}$	→0	0.021		100	100
$9/2^-_{qp_1} \rightarrow 7/2^-_{qp_1}$	1287→1075	2×10^{-5}	0.002		0.04
$\rightarrow 5/2^-_{qp_2}$	→809	0.0006			0.02
$\rightarrow 5/2^-_{qp_1}$	→191	0.048		100	100
$7/2^-_{qp_2} \rightarrow 9/2^-_{qp_1}$	1353→1287	0.005	0.025		0.02
$\rightarrow 7/2^-_{qp_1}$	→1075	0.002	0.011		0.7
$\rightarrow 3/2^-_{qp_3}$	→815	0.0004			0.04
$\rightarrow 5/2^-_{qp_2}$	→809	3×10^{-6}	0.060	13	30
$\rightarrow 5/2^-_{qp_1}$	→191	0.009	0.012	19	100
$\rightarrow 3/2^-_{qp_1}$	→0	0.010		100	100
$11/2^-_{qp_1} \rightarrow 7/2^-_{qp_2}$	2467→1353	0.001			0.8
$\rightarrow 9/2^-_{qp_1}$	→1287	0.006	0.001		8
$\rightarrow 7/2^-_{qp_1}$	→1075	0.039		100	100
$13/2^-_{qp_1} \rightarrow 11/2^-_{qp_1}$	2788→2467	0.0002	0.010		0.1
$\rightarrow 9/2^-_{qp_1}$	→1287	0.054		100	100
$15/2^-_{qp_1} \rightarrow 13/2^-_{qp_1}$	3736→2788	0.002	0.0007		2
$\rightarrow 11/2^-_{qp_1}$	→2467	0.033		100	100
$23/2^-_{bn_2} \rightarrow 21/2^-_{bn_1}$	6293→5943	0.007	0.001	1.3	2.5
$\rightarrow 19/2^-_{bn_1}$	→5466	0.013		100	100
$27/2^-_{bn_2} \rightarrow 23/2^-_{bn_2}$	7361→6293	0.015		100	100
$13/2^+_{qp_1} \rightarrow 11/2^+_{bn_1}$	3064→2813	0.000	0.000		
$\rightarrow 9/2^+_{qp_1}$	→2037	0.035		100	100
$11/2^+_{qp_1} \rightarrow 13/2^+_{qp_1}$	3173→3064	0.001	0.152		0.1
$\rightarrow 11/2^+_{bn_1}$	→2813	0.000	0.000		
$\rightarrow 9/2^+_{qp_1}$	→2037	0.034	0.080	100	100
$15/2^+_{bp_1} \rightarrow 11/2^+_{qp_1}$	3732→3173	0.003		10	28
$\rightarrow 13/2^+_{qp_1}$	→3064	0.002	0.001	100	100
$15/2^+_{bn_4} \rightarrow 15/2^+_{bp_1}$	3910→3732				
$\rightarrow 11/2^+_{qp_1}$	→3173				
$\rightarrow 13/2^+_{qp_1}$	→3064			15	
$\rightarrow 11/2^+_{bn_1}$	→2813	0.006		100	100
$17/2^+_{qp_1} \rightarrow 15/2^+_{bp_1}$	4122→3732	0.0006	0.003	0.8	0.5
$\rightarrow 13/2^+_{qp_1}$	→3064	0.048		100	100
$19/2^+_{bp_1} \rightarrow 17/2^+_{qp_1}$	4546→4122	0.00002	0.0001	9	0.2

TABLE III. (*Continued*).

$I_i^\pi \rightarrow I_f^\pi$ ($\hbar$) ($\hbar$)	$E_i \rightarrow E_f$ Expt. Expt.	$B(E2)(e^2b^2)$ IBFBPM	$B(M1)(\mu_N^2)$ IBFBPM	I_γ Expt.	IBFBPM
$\rightarrow 15/2^+_{bp_1}$	$\rightarrow 3732$	0.017		100	100
$21/2^+_{qp_1} \rightarrow 19/2^+_{bp_1}$	$5496 \rightarrow 4546$	0.00004	0.0007		0.4
$\rightarrow 17/2^+_{qp_1}$	$\rightarrow 4122$	0.043		100	100
$19/2^+_{qp_1} \rightarrow 21/2^+_{qp_1}$	$5714 \rightarrow 5496$	0.0007	0.234		1.6
$\rightarrow 19/2^+_{bp_1}$	$\rightarrow 4546$	0.00003	0.011		11
$\rightarrow 17/2^+_{qp_1}$	$\rightarrow 4122$	0.007	0.027	100	100
$\rightarrow 15/2^+_{bp_1}$	$\rightarrow 3732$	0.002			23
$25/2^+_{qp_1} \rightarrow 21/2^+_{qp_1}$	$6815 \rightarrow 5496$	0.026		60	60

the broken pair configurations $\pi\tilde{p}_{1/2}(\pi\tilde{p}_{3/2})^2$ and $\pi\tilde{f}_{5/2}(\pi\tilde{p}_{3/2})^2$ appear between 1.6 and 2.2 MeV. These configurations do not contribute to the higher-spin states near the yrast. The next structure, built on neutron broken pair configurations $\pi\tilde{p}_{3/2}(\nu\tilde{f}_{5/2})^2$ and $\pi\tilde{f}_{5/2}(\nu\tilde{f}_{5/2})^2$, is a group of states with spin $1/2^- - 11/2^-$ at $\approx 2.4-2.8$ MeV, while above them are the higher-spin states. The structure based on the $\pi\tilde{p}_{3/2}(\pi\tilde{f}_{5/2})^2$ configuration is also not relevant for high-spin states, being ≈ 1 MeV above the high-spin one-quasiproton states.

There are two additional negative parity broken pair structures that could be important. The $\pi\tilde{g}_{9/2}(\nu\tilde{f}_{5/2}\nu\tilde{g}_{9/2})$ one with its lowest lying high-spin $21/2^-$ state predicted at 6754 keV, and the ($\pi\tilde{p}_{3/2}$ and the $\pi\tilde{f}_{5/2}$)$(\pi\tilde{g}_{9/2})^2$ configurations generating lower spins above 7.2 MeV and higher spins ($23/2^-$ and $25/2^-$) at 8.78 MeV. Both structures are 1–2 MeV above the negative parity yrast and are not associated with the observed levels.

The only remaining negative parity broken pair configurations contributing to high-spin yrast states are the $\pi\tilde{p}_{3/2}(\nu\tilde{g}_{9/2})^2$ and $\pi\tilde{f}_{5/2}(\nu\tilde{g}_{9/2})^2$ ones. On the yrast they generate 100–200 keV separated doublets of the $19/2^-$, $23/2^-$, $25/2^-$, and $27/2^-$ states and a rather isolated $21/2^-$ state. On the basis of decay patterns we assign the $19/2^-_{bn_1}$, $21/2^-_{bn_1}$, $23/2^-_{bn_2}$, and $27/2^-_{bn_2}$ [predominantly based on $\pi\tilde{p}_{3/2}$, $\pi\tilde{f}_{5/2}$, $\pi\tilde{p}_{3/2}+\pi\tilde{f}_{5/2}$, and $\pi\tilde{f}_{5/2}$ proton quasiparticle states coupled to $(\nu\tilde{g}_{9/2})^2$, respectively] to the observed levels at 5466, 5943, 6293, and 7361 keV, respectively. Transitions in IBFBPM from $23/2^-_{bn_2}$ and $27/2^-_{bn_2}$ states to the calculated states that are not assigned to any observed levels are negligible. The $21/2^-_{bn_1} \rightarrow 19/2^-_{bn_1}$ transition is weak. The calculated reduced transition probabilities are: $B(E2)$ $(21/2^-_{bn_1} \rightarrow 19/2^-_{bn_1}) = 0.003$ (e^2b^2); $B(M1)$ $(21/2^-_{bn_1} \rightarrow 19/2^-_{bn_1}) = 0.009$ (μ_N^2). Since the $B(E2)$ values to the calculated $17/2^-$ states are also extremely small, the $21/2^-_{bn_1}$ state decays to the $19/2^+$ level at 4546 keV only because of the large transition energy. The IBFBPM calculation predicts that all possible $B(E2)$ and $B(M1)$ values in the decay of $19/2^-_{bn_1}$ to lower-lying $17/2^-$ and $15/2^-$ states are by many orders of magnitude hindered, and therefore this level is also forced to decay into positive parity levels.

The lowest energy positive parity level is the $9/2^+_{qp_1}$ one at 2037 keV, which is based on the $\pi\tilde{g}_{9/2}$ one-quasiproton state. At 2901 keV we predict a $5/2^+_{qp_1}\pi\tilde{g}_{9/2}$ core coupled state that was not observed in the present experiment. Since the occupation probability $v^2(\pi\tilde{g}_{9/2}) < 0.5$ and $\chi^\pi < 0$, the band structure based on the $\pi\tilde{g}_{9/2}$ configuration is of decoupled type, i.e., the lowest $11/2^+$ state of this structure lies above the corresponding $13/2^+$ state, both having strong and comparable transitions to the $9/2^+$ band head. The $11/2^{(+)}$ level at 2813 keV lying below the $13/2^+$ level and decaying predominantly to the $9/2^-_{qp_1}$ level, with a very weak branch to the $9/2^+$ level, evidently does not belong to the band based on the $\pi\tilde{g}_{9/2}$ configuration.

States based on the $\pi\tilde{p}_{1/2}$, $\pi\tilde{p}_{3/2}$, and $\pi\tilde{f}_{5/2}$ quasiparticle states coupled to the neutron broken pair $(\nu\tilde{f}_{5/2}\nu\tilde{g}_{9/2})$ appear in our calculation above ≈ 3 MeV, with members up to spin $19/2^+$. The $19/2^+$ member of this structure is predicted at 3461 keV, i.e., below the observed yrast states. States with higher spins built on this configuration are also predicted to lie 0.5–0.8 MeV below the members of the $\pi\tilde{g}_{9/2}$ one-quasiproton band. Our calculation cannot prove that unobserved high-spin states based on this broken pair configuration are on the yrast due to the following arguments:

(1) The nature of this structure forbids or at least highly hinders transitions from other families of levels into these states.

(2) States based on this configuration do not show a distinct band structure. The $\pi\tilde{p}_{1/2}$, $\pi\tilde{p}_{3/2}$, and $\pi\tilde{f}_{5/2}$ components are fragmented in wave functions, resulting in a high level density above 3 MeV, and therefore even transitions between members of this family are extremely weak.

(3) The effective core for a negative parity broken pair at high excitation energy could be different from the core that influences the one-quasiproton band, shifting this broken pair configuration above the yrast.

Therefore, we can conclude that it is possible that, although the calculated positive parity yrast states are ≈ 0.5 MeV below the observed yrast levels, they cannot be populated from the observed levels. The lowest state of this neutron broken pair configuration is the calculated $11/2^+_{bn_1}$ state. We assign it to the 2813 keV level. The only state having a sizeable transition into it is the calculated $15/2^+_{bn_4}$ state based on the same fermion configuration [$B(E2)(15/2^+_{bn_4}$

$\rightarrow 11/2^+_{\mathrm{bn}_1}) = 0.006\ e^2\mathrm{b}^2$]. We tentatively assign $15/2^+_{\mathrm{bn}_4}$ to the level at 3910 keV.

An important three-quasiproton configuration, the $\pi\tilde{g}_{9/2}(\pi\tilde{p}_{3/2}\pi\tilde{f}_{5/2})$ one, appears above 4 MeV. Among the relevant high-spin states, the $15/2^+$, $19/2^+$, and $23/2^+$ states based on this broken pair structure are below the corresponding one-quasiproton states. We associate the $15/2^+_{14}$ and $19/2^+_{18}$ IBFBPM states with the observed levels at 3732 and 4546 keV. As mentioned previously, the other $15/2^+$ and $19/2^+$ states below are based on neutron pairs. Therefore, we shall label the 3732 and 4546 keV levels by $15/2^+_{\mathrm{bp}_1}$ and $19/2^+_{\mathrm{bp}_1}$. In Table III the transitions from $15/2^+_{\mathrm{bp}_1}$ to $11/2^+_{\mathrm{bn}_1}$ and $13/2^-_{\mathrm{qp}_1}$ are omitted, as in the present version of IBFBPM they cannot be calculated. The strong transition to the $13/2^-_{\mathrm{qp}_1}$ state can be attributed to the components based on $(\nu\tilde{f}_{5/2}\nu\tilde{g}_{9/2})$ in the wave function of $15/2^+_{\mathrm{bp}_1}$.

Levels at 3064, 3173, 4122, 5496, 5714, and 6815 keV are assigned to the $13/2^+_1$, $11/2^+_2$, $17/2^+_6$, $21/2^+_6$, $19/2^+_{22}$, and $25/2^+_3$ (i.e., $13/2^+_{\mathrm{qp}_1}$, $11/2^+_{\mathrm{qp}_1}$, $17/2^+_{\mathrm{qp}_1}$, $21/2^+_{\mathrm{qp}_1}$, $19/2^+_{\mathrm{qp}_1}$, and $25/2^+_{\mathrm{qp}_1}$) members of the $\pi\tilde{g}_{9/2}$ one-quasiproton band, respectively. The strong $E2$ transition of 899 keV from the 6815 keV state does not correspond to any of the calculated transitions, therefore we are not able to assign an IBFBPM state to the 5916 keV $21/2^+$ level fed by it.

Transitions from the levels with $\pi\tilde{p}_{3/2}(\nu\tilde{g}_{9/2})^2$ and $\pi\tilde{f}_{5/2}(\nu\tilde{g}_{9/2})^2$ configurations are forbidden or highly hindered in leading order to the $19/2^+$ level at 4546 keV, based on the $\pi\tilde{g}_{9/2}(\pi\tilde{p}_{3/2}\pi\tilde{f}_{5/2})$ configuration, and also to other positive parity levels containing this dominant configuration, as well as to those states, which are predominantly $\pi\tilde{g}_{9/2}$ core coupled states. Strong $E1$ transitions are possible if $\nu\tilde{f}_{7/2}$ components are present in positive parity final states. In order to keep the size of configuration space manageable, the $\nu\tilde{f}_{7/2}$ states have been omitted from the present calculation. Nevertheless, we have performed an IBFBPM calculation with $\nu\tilde{f}_{7/2}$ included in the configuration space, but the boson space was reduced. The energy of the $\nu\tilde{f}_{7/2}$ quasiparticle was taken 3.7 MeV above the Fermi level. In this schematic calculation we obtained $17/2^+$ and $19/2^+$ states as members of the lowest-lying structure containing the $\nu\tilde{f}_{7/2}$ state, in the $\pi\tilde{p}_{3/2}(\nu\tilde{f}_{7/2}\nu\tilde{g}_{9/2})$ configuration, at ≈ 5.5 MeV, i.e., at the calculated energy of the $\pi\tilde{g}_{9/2}(\pi\tilde{p}_{3/2}\pi\tilde{f}_{5/2})$ states in the realistic calculations. Therefore, we conclude that $17/2^+$,$19/2^+$, and other positive parity levels (including the 4546 keV level) above 4 MeV should have additional $\pi\tilde{p}_{3/2}(\nu\tilde{f}_{7/2}\nu\tilde{g}_{9/2})$ components that enable $E1$ transitions from $(\nu\tilde{g}_{9/2})^2$ levels. The residual interaction between broken proton and neutron pairs could lower the calculated energy of states containing both types of pairs, in agreement with the rather low energy of the 4546 keV $19/2^+$ level. The present version of IBFBPM cannot account for states containing both types of pairs.

We note that the $\pi\tilde{g}_{9/2}(\pi\tilde{p}_{3/2})^2$ broken pair configuration appearing at 3.7–3.9 MeV does not generate high-spin states near the yrast, nor does the $\pi\tilde{g}_{9/2}(\pi\tilde{f}_{5/2})^2$ one (with high-spin states ≈ 1 MeV above the observed one-quasiproton levels) or the $(\pi\tilde{g}_{9/2})^3$ one being active above 10 MeV. The IBFBPM calculation predicts the lowest $25/2^+$ state based on $\pi\tilde{g}_{9/2}(\nu\tilde{g}_{9/2})^2$ at 7336 keV. This level was not populated in the present experiment.

VI. CALCULATION FOR ^{67}Ga IN IBFBPM

The core nucleus for ^{67}Ga is $^{66}_{30}\mathrm{Zn}_{36}$. Here we use the parametrization from Ref. [38]: $h_1 = 1.039$, $h_2 = 0$, $h_3 = 0$, $h_{40} = 0.147$, $h_{42} = -0.2292$, $h_{44} = 0.5595$ (all h_i parameters in MeV) and the total boson number $N = 5$.

From Ref. [38] the boson-fermion interaction strengths for protons are: $\Gamma_0^\pi = 0.4$ MeV, $\Lambda_0^\pi = 0.5$ MeV. Only the monopole strength $A_0^\pi = 0$ MeV is slightly adjusted to the high-spin data.

Starting from the same single-particle energies and pairing strength for neutrons as in ^{65}Ga and lowering the $E(\nu\tilde{g}_{9/2})$ by 0.4 MeV, we obtain $E(\nu\tilde{f}_{5/2}) = 1.42$ MeV, $E(\nu\tilde{p}_{3/2}) = 1.80$ MeV, $E(\nu\tilde{p}_{1/2}) = 2.00$ MeV, $E(\nu\tilde{g}_{9/2}) = 2.42$ MeV, $v^2(\nu\tilde{f}_{5/2}) = 0.60$, $v^2(\nu\tilde{p}_{3/2}) = 0.82$, $v^2(\nu\tilde{p}_{1/2}) = 0.14$, $v^2(\nu\tilde{g}_{9/2}) = 0.07$. All other parameters are the same as in the calculations for ^{65}Ga.

In Fig. 8 we present the calculated energy spectrum of ^{67}Ga in comparison to the available data and in Table IV the calculated $E2$ and $M1$ transitions are compared with the experimental branching ratios. Altogether branchings from 27 states were analyzed. Similar to the case in ^{65}Ga, all the transitions predicted to be strong were found, or are below the detection limit, except the $17/2^+_{\mathrm{bp}_2} \rightarrow 15/2^+_{\mathrm{bp}_1}$ transition, which is at least a factor of 20 weaker than expected. All the transitions predicted to be weak are weak or not seen, although, the $17/2^-_{\mathrm{qp}_1} \rightarrow 15/2^-_{\mathrm{qp}_1}$ and the $7/2^-_{\mathrm{qp}_2} \rightarrow 3/2^-_{\mathrm{qp}_1}$ transitions are much stronger than expected.

One-quasiproton negative parity states in ^{67}Ga correspond to their counterparts in ^{65}Ga, with the exception of the $17/2^-_{\mathrm{qp}_1}$ state that is observed in ^{67}Ga, in agreement with the IBFBPM prediction. Therefore, we associate the $3/2^-_{\mathrm{qp}_1}$, $1/2^-_{\mathrm{qp}_1}$, $5/2^-_{\mathrm{qp}_1}$, $3/2^-_{\mathrm{qp}_2}$, $5/2^-_{\mathrm{qp}_2}$, $1/2^-_{\mathrm{qp}_2}$, $7/2^-_{\mathrm{qp}_1}$, $7/2^-_{\mathrm{qp}_2}$, $9/2^-_{\mathrm{qp}_1}$, $11/2^-_{\mathrm{qp}_1}$, $13/2^-_{\mathrm{qp}_1}$, $15/2^-_{\mathrm{qp}_1}$, and $17/2^-_{\mathrm{qp}_1}$ IBFBPM states, with the observed levels at 0, 167, 359, 828, 911, 1082, 1202, 1412, 1519, 2653, 3160, 4280, and 4750 keV, respectively. Compared to the corresponding states in ^{65}Ga, some states have different dominant components in their wave functions. The $3/2^-_{\mathrm{qp}_2}$, $7/2^-_{\mathrm{qp}_1}$, $11/2^-_{\mathrm{qp}_1}$, and $15/2^-_{\mathrm{qp}_1}$ states are based mainly on $\pi\tilde{p}_{3/2}$ and $7/2^-_{\mathrm{qp}_2}$ is based on the $\pi\tilde{f}_{5/2}$ quasiproton state. We note that the $11/2^-_{\mathrm{qp}_1}$ and $15/2^-_{\mathrm{qp}_1}$ states are negligible above the calculated yrast states. For negative parity, broken pair configurations do not exhibit sizeable differences with respect to ^{65}Ga. As in the lighter isotope, the observed high-spin negative parity states above 5 MeV are based on $\pi\tilde{p}_{3/2}(\nu\tilde{g}_{9/2})^2$ and $\pi\tilde{f}_{5/2}(\nu\tilde{g}_{9/2})^2$, with the two lowest members of this structure, $19/2^-_{\mathrm{bn}_1}$ and $21/2^-_{\mathrm{bn}_1}$, assigned to the levels at 5085 and 5225 keV, respectively. Above these states, we assigned the IBFBPM $21/2^-_{\mathrm{bn}_2}$, $23/2^-_{\mathrm{bn}_1}$,

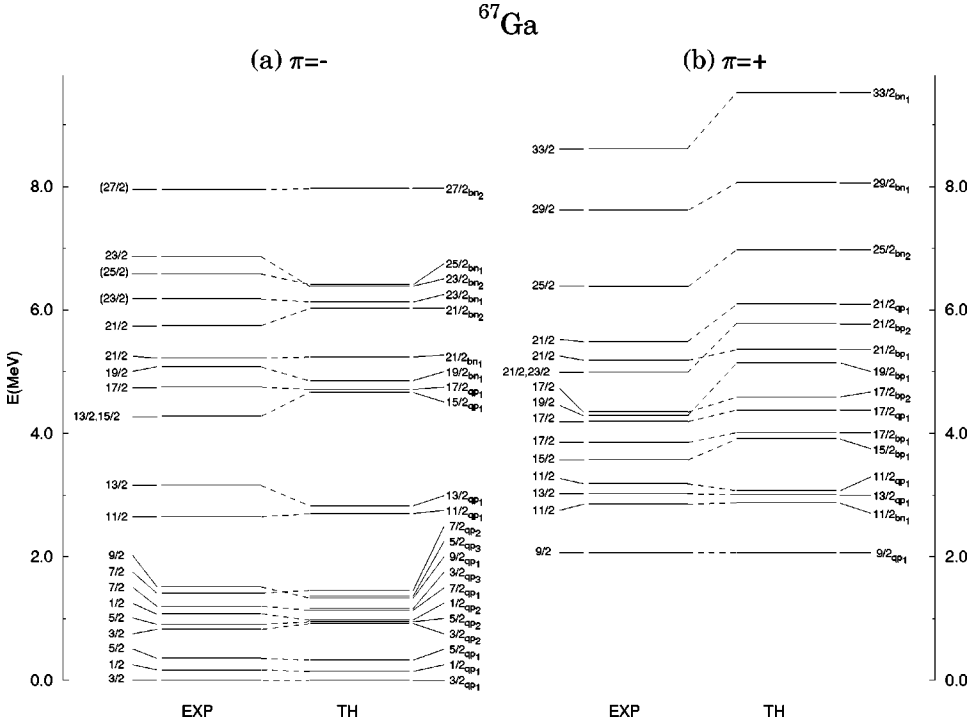

FIG. 8. Calculated states in ^{67}Ga of (a) negative parity and (b) positive parity, in comparison to the available data. Below 1.50 MeV of excitation energy all calculated states are shown, and above 1.50 MeV only those that have experimental counterparts. Calculated states are tentatively assigned to the experimental levels (see text for discussion).

$25/2^-_{\mathrm{bn}_1}$, $23/2^-_{\mathrm{bn}_2}$, and $27/2^-_{\mathrm{bn}_2}$ states to the 5744, 6185, 6589, 6870, and 7958 keV levels, respectively.

The positive parity spectrum of ^{67}Ga exhibits some differences with respect to ^{65}Ga. Levels that have evident counterparts are

(1) Members of the $\pi\tilde{g}_{9/2}$ one-quasiproton band $9/2^+_1$, $13/2^+_4$, and $11/2^+_6$. We labeled these states (due to reasons discussed in the case of ^{65}Ga in connection to high density of levels based on neutron broken pairs above 3 MeV) as $9/2^+_{\mathrm{qp}_1}$, $13/2^+_{\mathrm{qp}_1}$, and $11/2^+_{\mathrm{qp}_1}$. These states correspond to the 2073, 3031, and 3190 keV levels, respectively.

(2) The level at 2862 keV, assigned to the IBFBPM $11/2^+_{\mathrm{bn}_1}$ state which is based on the neutron broken pair $(\nu\tilde{f}_{5/2}\nu\tilde{g}_{9/2})$ configuration.

(3) Levels at 3577 and 4290 keV, associated with the calculated $15/2^+_{14}$ and $19/2^+_{12}$ states (labeled as $15/2^+_{\mathrm{bp}_1}$ and $19/2^+_{\mathrm{bp}_1}$). They are members of the $\pi\tilde{g}_{9/2}(\pi\tilde{p}_{3/2}\pi\tilde{f}_{5/2})$ broken pair structure.

The main difference with respect to ^{65}Ga is due to the $17/2^+$ and $21/2^+$ levels. Electromagnetic transitions from and into these levels, as well as their pattern, can be associated with an interplay of $\pi\tilde{g}_{9/2}$, $\pi\tilde{g}_{9/2}(\pi\tilde{p}_{3/2}\pi\tilde{f}_{5/2})$, and $\pi\tilde{g}_{9/2}(\pi\tilde{f}_{5/2})^2$ components in the wave functions of these levels. The $17/2^+_{12}$ and $21/2^+_{16}$ states (labeled as $17/2^+_{\mathrm{qp}_1}$ and $21/2^+_{\mathrm{qp}_1}$) are based predominantly on $\pi\tilde{g}_{9/2}$ and are associated with 4198 and 5491 keV levels, respectively. The levels at 3855, 4349, 4995, and 5186 keV, with dominant three-quasiproton components, are assigned to the $17/2^+_7$, $17/2^+_{20}$, $21/2^+_9$, and $21/2^+_5$ IBFBPM states (labeled as $17/2^+_{\mathrm{bp}_1}$, $17/2^+_{\mathrm{bp}_2}$, $21/2^+_{\mathrm{bp}_2}$, and $21/2^+_{\mathrm{bp}_1}$, respectively).

Calculations in IBFBPM predict that positive parity yrast levels above 6 MeV are based on $\pi\tilde{g}_{9/2}(\nu\tilde{g}_{9/2})^2$. The calculated $25/2^+_{\mathrm{bn}_2}$, $29/2^+_{\mathrm{bn}_1}$, and $33/2^+_{\mathrm{bn}_1}$ states, belonging to this structure, are assigned to the 6379, 7619, and 8616 keV levels.

VII. CONCLUSION

The experimental level schemes of ^{65,67}Ga have been significantly extended. While the existence, as well as spin and parity values of the states below 3.5–4.0 MeV were confirmed, the experimental information on the high-spin states has been doubled concerning the number of γ rays, the number of levels, and the amount of spin assignments by adding 15–20 new levels in the 3.5–7.0 MeV region. As a result of these investigations 1–3 additional states could be observed above the yrast in the spin 15/2–23/2 region.

The present calculation of nuclear structure of ^{65,67}Ga reveals an interplay of one- and three-quasiparticle states in the framework of the interacting boson-fermion model. In both nuclei the negative parity states observed below $\approx$4 MeV were assigned to quasiparticle+phonon states, above it the proton quasiparticles and the phonons are coupled to a completely aligned pair of neutrons in the yrast states. The positive parity sequence of the $\pi g_{9/2}$ + phonon excitations could be revealed up to spin 25/2 and 21/2 in ^{65}Ga and ^{67}Ga, respectively. Between 3.5 and 5.5 MeV a set of three proton states could be identified in ^{67}Ga, while the high-spin yrast sequence is based on the aligned $g_{9/2}$ neutron configuration as in the case of negative parity states. In ^{65}Ga only a pair of broken proton states could be identified. Although, in both

TABLE IV. Calculated $E2$ and $M1$ transitions for ^{67}Ga in comparison to data. Experimental I_γ values for transitions that are not observed in the present experiment are from Ref. [15].

$I_i^\pi \rightarrow I_f^\pi$ ($\hbar$) ($\hbar$)	$E_i \rightarrow E_f$ Expt. Expt.	$B(E2)(e^2\mathrm{b}^2)$ IBFBPM	$B(M1)(\mu_N^2)$ IBFBPM	I_γ Expt.	I_γ IBFBPM
$1/2^-_{qp_1} \rightarrow 3/2^-_{qp_1}$	167→0	0.013	0.058	100	100
$5/2^-_{qp_1} \rightarrow 1/2^-_{qp_1}$	359→167	0.027			1.8
$\rightarrow 3/2^-_{qp_1}$	→0	0.003	0.006	100	100
$3/2^-_{qp_2} \rightarrow 5/2^-_{qp_1}$	828→359	1×10^{-5}	0.013	4	6
$\rightarrow 1/2^-_{qp_1}$	→167	2×10^{-5}	0.022	10	27
$\rightarrow 3/2^-_{qp_1}$	→0	0.027	0.028	100	100
$5/2^-_{qp_2} \rightarrow 3/2^-_{qp_2}$	911→828	0.002	0.306		0.9
$\rightarrow 5/2^-_{qp_1}$	→359	9×10^{-5}	0.0005	2.2	0.5
$\rightarrow 1/2^-_{qp_1}$	→167	0.003		2.2	2.0
$\rightarrow 3/2^-_{qp_1}$	→0	0.029	0.010	100	100
$1/2^-_{qp_2} \rightarrow 5/2^-_{qp_2}$	1082→911	0.0004			0.0002
$\rightarrow 3/2^-_{qp_2}$	→828	0.0003	0.533	12	37
$\rightarrow 5/2^-_{qp_1}$	→359	0.003			1.7
$\rightarrow 1/2^-_{qp_1}$	→167		0.030	100	100
$\rightarrow 3/2^-_{qp_1}$	→0	0.021	0.005	33	122
$7/2^-_{qp_1} \rightarrow 5/2^-_{qp_2}$	1202→911	0.002	0.131		6
$\rightarrow 3/2^-_{qp_2}$	→828	0.0004			0.0004
$\rightarrow 5/2^-_{qp_1}$	→359	0.002	0.012	31	14
$\rightarrow 3/2^-_{qp_1}$	→0	0.033		100	100
$7/2^-_{qp_2} \rightarrow 7/2^-_{qp_1}$	1412→1202	0.002	0.002		0.06
$\rightarrow 5/2^-_{qp_2}$	→911	0.002	0.011	20	5
$\rightarrow 3/2^-_{qp_2}$	→828	0.001			0.2
$\rightarrow 5/2^-_{qp_1}$	→359	0.024	0.008	100	100
$\rightarrow 3/2^-_{qp_1}$	→0	3×10^{-5}		20	0.3
$9/2^-_{qp_1} \rightarrow 7/2^-_{qp_2}$	1519→1412	0.003	0.018		0.03
$\rightarrow 7/2^-_{qp_1}$	→1202	0.0007	0.005		0.2
$\rightarrow 5/2^-_{qp_2}$	→911	0.0003			0.02
$\rightarrow 5/2^-_{qp_1}$	→359	0.049		100	100
$11/2^-_{qp_1} \rightarrow 9/2^-_{qp_1}$	2653→1519	0.001	0.007		5
$\rightarrow 7/2^-_{qp_2}$	→1412	0.0004			0.4
$\rightarrow 7/2^-_{qp_1}$	→1202	0.051		100	100
$13/2^-_{qp_1} \rightarrow 11/2^-_{qp_1}$	3160→2653	0.0003	0.004		0.1
$\rightarrow 9/2^-_{qp_1}$	→1519	0.065		100	100
$15/2^-_{qp_1} \rightarrow 13/2^-_{qp_1}$	4280→3160	0.0009	0.004		1.5
$\rightarrow 11/2^-_{qp_1}$	→2653	0.056		100	100
$17/2^-_{qp_1} \rightarrow 15/2^-_{qp_1}$	4750→4280	8×10^{-5}	0.002	12	0.04
$\rightarrow 13/2^-_{qp_1}$	→3160	0.067		100	100
$21/2^-_{bn_2} \rightarrow 21/2^-_{bn_1}$	5744→5225	2×10^{-6}	0.003	100	100
$\rightarrow 19/2^-_{bn_1}$	→5085	0.0003	0.002	24	161
$23/2^-_{bn_1} \rightarrow 21/2^-_{bn_2}$	6185→5744	0.0004	0.718	30	89
$\rightarrow 21/2^-_{bn_1}$	→5225	0.0007	0.007		10
$\rightarrow 19/2^-_{bn_1}$	→5085	0.025		40	40
$25/2^-_{bn_1} \rightarrow 23/2^-_{bn_1}$	6589→6185	0.0006	0.006		0.4
$\rightarrow 21/2^-_{bn_2}$	→5744	8×10^{-6}			0.002
$\rightarrow 21/2^-_{bn_1}$	→5225	0.036		100	100
$23/2^-_{bn_2} \rightarrow 25/2^-_{bn_1}$	6870→6589	0.007	0.598		20
$\rightarrow 23/2^-_{bn_1}$	→6185	0.0002	0.0004		0.2
$\rightarrow 21/2^-_{bn_2}$	→5744	4×10^{-5}	0.003	36	6
$\rightarrow 21/2^-_{bn_1}$	→5225	0.008	0.0003	100	100
$\rightarrow 19/2^-_{bn_1}$	→5085	3×10^{-7}			0.005

TABLE IV. (*Continued*).

$I_i^\pi \rightarrow I_f^\pi$ ($\hbar$) ($\hbar$)	$E_i \rightarrow E_f$ Expt. Expt.	$B(E2)(e^2b^2)$ IBFBPM	$B(M1)(\mu_N^2)$ IBFBPM	I_γ Expt.	I_γ IBFBPM
$27/2^-_{bn_2} \rightarrow 23/2^-_{bn_2}$	7958→6870	0.041		50	259
$\rightarrow 25/2^-_{bn_1}$	→6589	0.005	0.0001	100	100
$\rightarrow 23/2^-_{bn_1}$	→6185	9×10^{-6}			0.6
$13/2^+_{qp_1} \rightarrow 9/2^+_{qp_1}$	3031→2073	0.037		100	100
$11/2^+_{qp_1} \rightarrow 13/2^+_{qp_1}$	3190→3031	0.001	0.119		0.4
$\rightarrow 9/2^+_{qp_1}$	→2073	0.041	0.058	100	100
$15/2^+_{bp_1} \rightarrow 11/2^+_{qp_1}$	3577→3190	0.002		3.4	33
$\rightarrow 13/2^+_{qp_1}$	→3031	0.0009	4×10^{-5}	100	100
$17/2^+_{bp_1} \rightarrow 15/2^+_{bp_1}$	3855→3577	0.006	0.039	1.2	22
$\rightarrow 13/2^+_{qp_1}$	→3031	0.015		100	100
$17/2^+_{qp_1} \rightarrow 17/2^+_{bp_1}$	4198→3855	6×10^{-5}	0.095	90	6
$\rightarrow 15/2^+_{bp_1}$	→3577	0.001	0.028		11
$\rightarrow 13/2^+_{qp_1}$	→3031	0.043		100	100
$19/2^+_{bp_1} \rightarrow 17/2^+_{qp_1}$	4290→4198	0.002	0.001		0.02
$\rightarrow 17/2^+_{bp_1}$	→3855	0.004	9×10^{-5}	1.6	1.2
$\rightarrow 15/2^+_{bp_1}$	→3577	0.029		100	100
$17/2^+_{bp_2} \rightarrow 19/2^+_{bp_1}$	4349→4290	6×10^{-5}	0.004		0.02
$\rightarrow 17/2^+_{qp_1}$	→4198	3×10^{-5}	0.008		0.8
$\rightarrow 17/2^+_{bp_1}$	→3855	0.0004	0.001	52	5
$\rightarrow 15/2^+_{bp_1}$	→3577	0.0001	0.012	<10	146
$\rightarrow 13/2^+_{qp_1}$	→3031	0.0014		100	100
$21/2^+_{bp_2} \rightarrow 17/2^+_{bp_2}$	4995→4349	0.035			24
$\rightarrow 19/2^+_{bp_1}$	→4290	2×10^{-5}	0.033	100	100
$\rightarrow 17/2^+_{qp_1}$	→4198	0.009			17
$\rightarrow 17/2^+_{bp_1}$	→3855	0.0002			2.7
$21/2^+_{bp_1} \rightarrow 21/2^+_{bp_2}$	5186→4995	0.0002	0.005		0.03
$\rightarrow 17/2^+_{bp_2}$	→4349	0.0002			0.04
$\rightarrow 19/2^+_{bp_1}$	→4290	0.003	0.106	31	67
$\rightarrow 17/2^+_{qp_1}$	→4198	0.0003			0.2
$\rightarrow 17/2^+_{bp_1}$	→3855	0.040		100	100
$21/2^+_{qp_1} \rightarrow 21/2^+_{bp_1}$	5491→5186	0.0002	0.029	2.1	0.7
$\rightarrow 21/2^+_{bp_2}$	→4995	1×10^{-5}	0.001		0.1
$\rightarrow 17/2^+_{bp_2}$	→4349	0.008		27	9
$\rightarrow 19/2^+_{bp_1}$	→4290	0.0004	0.004		7
$\rightarrow 17/2^+_{qp_1}$	→4198	0.048		100	100
$\rightarrow 17/2^+_{bp_1}$	→3855	0.002		67	14

^{65,67}Ga there are positive parity states which could be assigned to a broken low-spin neutron pair + proton configuration, this set of states remains problematic. This group of states is predicted to be yrast in the spin 11/2–23/2 range, which is not the case. These states might be weakly connected to the rest of the level scheme, or the core may be somewhat different for different families of broken pair configurations, resulting in additional energy shifts between these families of states. Such an energy difference is often present, e.g., in total routhian surface calculations. In spite of the above-mentioned problems, the general agreement between the present IBFBPM calculation and experiment is reasonable. For a majority of the observed levels we proposed the dominant configuration in the wave function on the basis of comparison of their electromagnetic properties with the experimental ones. It is important that not only the energies, but also the branching ratios could be described at least in a qualitative way. The main branches were always calculated to be strong, and the strength of the side branches were estimated with a precision better than an order of magnitude in most cases, making possible the assignment of most of the states.

ACKNOWLEDGMENTS

This work was supported by the Swedish and Danish Natural Science Research Councils, and the Hungarian Fund for Science Research (OTKA Contract No. 20655).

[1] R. Almar, O. Civitarese, F. Krmpotič, and J. Navaza, Phys. Rev. C **6**, 187 (1972).
[2] V. Paar, Nucl. Phys. **A211**, 29 (1973).
[3] D. Vretenar, G. Bonsignori, and M. Savoia, Z. Phys. A **351**, 289 (1995).
[4] C. Rossi Alvarez *et al.*, Phys. Rev. C **54**, 57 (1996).
[5] M.G. Betigeri, H.H. Duhm, R. Santo, R. Stock, and R. Bock, Nucl. Phys. **A100**, 416 (1967); R.G. Couch, J.A. Biggerstaff, F.G. Perey, S. Raman, and K.K. Seth, Phys. Rev. C **2**, 149 (1970); M.G. Betigeri, P. David, J. Debrus, H. Mommsen, and A. Riccato, Nucl. Phys. **A171**, 401 (1971); B. Zeidman, R.H. Siemssen, G.C. Morrison, and L.L. Lee, Phys. Rev. C **9**, 409 (1974).
[6] H.W. Jongsma, J.C. De Lange, H. Verheul, F.W.N. de Boer, and P.F.A. Goudsmit, Z. Phys. **262**, 247 (1973).
[7] H. Bakhru and I.M. Ladenbauer-Bellis, Phys. Rev. **177**, 1686 (1969); W.H. Zoller, G.E. Gordon, and W.B. Walters, Nucl. Phys. **A137**, 606 (1969).
[8] E. Finckh, U. Jahncke, B. Schreiber, and A. Weidinger, Nucl. Phys. **A144**, 67 (1970); W.T. Bass and P.H. Stelson, Phys. Rev. C **2**, 2154 (1970).
[9] L. Harms-Ringdahl, J. Sztarkier, and Z.P. Sawa, Phys. Scr. **9**, 15 (1974); T. Paradellis, Nucl. Phys. **A279**, 293 (1977); A.M. Al-Naser, A.H. Behbehani, L.L. Green, C.J. Lister, P.J. Nolan, and J.F. Sharpey-Schafer, J. Phys. G **3**, 1383 (1977); C. Rangacharyulu, I.M. Szoghy, C. St-Pierre, and K. Ramavataram, Can. J. Phys. **57**, 733 (1979); C. Rangacharyulu, M.B. Chatterjee, C. Pruneau, and C. St-Pierre, *ibid.* **60**, 815 (1982); P. Banerjee, B. Sethi, M.B. Chatterjee, and R. Goswami, Nuovo Cimento A **110**, 1365 (1997).
[10] H. Kawakami, A.P. de Lima, R.M. Ronningen, A.V. Ramayya, J.H. Hamilton, R.L. Robinson, H.J. Kim, and L.K. Peker, Phys. Rev. C **21**, 1311 (1980).
[11] A.M. Al-Naser, A.H. Behbehani, L.L. Green, A.N. James, C.J. Lister, P.J. Nolan, N. Rammo, J.F. Sharpey-Schafer, L. Zybert, and R. Zybert, J. Phys. G **10**, 1611 (1978).
[12] V. Zobel, L. Cleemann, J. Eberth, W. Neumann, and N. Wiehl, Nucl. Phys. **A316**, 165 (1979).
[13] S. Zhu *et al.*, Chin. J. Nucl. Phys. **13**, 331 (1991).
[14] M.R. Bhat, Nucl. Data Sheets **69**, 209 (1993).
[15] M.R. Bhat, Nucl. Data Sheets **64**, 875 (1991).
[16] H. Grawe *et al.*, Z. Phys. A **358**, 185 (1997).
[17] B. Herskind, Nucl. Phys. **A447**, 395c (1985).
[18] G. Sletten, *Proceedings of the International Seminar on The Frontier of Nuclear Spectroscopy*, Kyoto, 1992 (World Scientific, Singapore, 1993).
[19] T. Kuroyanagi *et al.*, Nucl. Instrum. Methods Phys. Res. A **A316**, 289 (1992).
[20] S. E. Arnell, H. A. Roth, Ö. Skeppstedt, J. Bialkowski, M. Moszýnski, D. Wolski, and J. Nyberg, Nucl. Instrum. Methods Phys. Res. A **300**, 303 (1991).
[21] D. Wolski, M. Moszýnski, T. Ludziejewski, A. Johnson, W. Klamra, and Ö. Skeppstedt, Nucl. Instrum. Methods Phys. Res. A **360**, 584 (1995).
[22] A. Johnson *et al.*, Nucl. Phys. **A557**, 401c (1993).
[23] D. C. Radford, Nucl. Instrum. Methods Phys. Res. A **361**, 290 (1995).
[24] M. Palacz, Ph.D. thesis, University of Warsaw, 1997; M. Palacz *et al.*, Nucl. Phys. **A627**, 162 (1997).
[25] S. Törmänen, Ph.D. thesis, University of Jyväskylä, 1996.
[26] F. Iachello and A. Arima, *The Interacting Boson Model* (Cambridge University Press, Cambridge, 1987).
[27] A. Arima and F. Iachello, Phys. Rev. Lett. **35**, 1069 (1975); Ann. Phys. (N.Y.) **99**, 253 (1976); **111**, 201 (1978); **123**, 468 (1979).
[28] F. Iachello and O. Scholten, Phys. Rev. Lett. **43**, 679 (1979).
[29] F. Iachello and P. Van Isacker, *The Interacting Boson Fermion Model* (Cambridge University Press, Cambridge, 1991).
[30] O. Scholten, Prog. Part. Nucl. Phys. **14**, 189 (1985).
[31] V. Paar, in *Capture Gamma-Ray Spectroscopy and Related Topics*, edited by S. Raman, AIP Conf. Proc. No. 125 (AIP, New York, 1985), p. 70.
[32] S. Brant, V. Paar, and D. Vretenar, Z. Phys. A **319**, 355 (1984); V. Paar, D.K. Sunko, and D. Vretenar, *ibid.* **327**, 291 (1987).
[33] F. Iachello and D. Vretenar, Phys. Rev. C **43**, 945 (1991).
[34] D. Vretenar, V. Paar, G. Bonsignori, and M. Savoia, Phys. Rev. C **42**, 993 (1990); **44**, 223 (1991).
[35] D. Vretenar, G. Bonsignori, and M. Savoia, Phys. Rev. C **47**, 2019 (1993).
[36] C.J. Lister, P. Chowdhury, and D. Vretenar, Nucl. Phys. **A557**, 361 (1993).
[37] Y. Tokunaga *et al.*, Nucl. Phys. **A430**, 269 (1984).
[38] J. Timár, T. X. Quang, Zs. Dombrádi, T. Fényes, A. Krasznahorkay, S. Brant, V. Paar, and Lj. Šimičić, Nucl. Phys. **A552**, 170 (1993).
[39] J. Timár, T. X. Quang, T. Fényes, Zs. Dombrádi, A. Krasznahorkay, J. Kumpulainen, R. Julin, S. Brant, V. Paar, and Lj. Šimičić, Nucl. Phys. **A573**, 61 (1994).
[40] A. Algora, D. Sohler, T. Fényes, Z. Gácsi, S. Brant, and V. Paar, Nucl. Phys. **A588**, 399 (1995).
[41] T. Fényes, A. Algora, Zs. Podolyák, D. Sohler, J. Timár, S. Brant, V. Paar, and Lj. Šimičić, Fiz. Elem. Chastits At. Yadra **26**, 831 (1995).
[42] D. Sohler, A. Algora, T. Fényes, J. Gulyás, S. Brant, and V. Paar, Nucl. Phys. **A604**, 25 (1996).
[43] D. Sohler *et al.*, Z. Phys. A **357**, 239 (1997).
[44] D. Sohler, Zs. Podolyák, J. Gulyás, T. Fényes, A. Algora, Zs. Dombrádi, S. Brant, and V. Paar, Nucl. Phys. **A618**, 35 (1997).
[45] D. Sohler *et al.* (unpublished).
[46] L.S. Kisslinger and R.A. Sorensen, Rev. Mod. Phys. **35**, 853 (1963).
[47] B.S. Reehal and R.A. Sorensen, Phys. Rev. C **2**, 819 (1970).
[48] T. Paradellis and S. Hontzeas, Can. J. Phys. **49**, 1750 (1971).
[49] G. de Angelis, M.A. Cardona, M. de Poli, S. Lunardi, D. Bazzacco, F. Brandolini, D. Vretenar, G. Bonsignori, M. Savoia, and R. Wyss, Phys. Rev. C **49**, 2990 (1994).
[50] C.M. Petrache *et al.*, Nucl. Phys. **A617**, 228 (1997).